

University of Montana

ScholarWorks at University of Montana

Graduate Student Theses, Dissertations, &
Professional Papers

Graduate School

1983

Kinematic interpretation of mylonitic rocks in Okanogan dome north-central Washington and implications for dome evolution

Vicki L. Hansen
The University of Montana

Follow this and additional works at: <https://scholarworks.umt.edu/etd>

Let us know how access to this document benefits you.

Recommended Citation

Hansen, Vicki L., "Kinematic interpretation of mylonitic rocks in Okanogan dome north-central Washington and implications for dome evolution" (1983). *Graduate Student Theses, Dissertations, & Professional Papers*. 7442.

<https://scholarworks.umt.edu/etd/7442>

This Thesis is brought to you for free and open access by the Graduate School at ScholarWorks at University of Montana. It has been accepted for inclusion in Graduate Student Theses, Dissertations, & Professional Papers by an authorized administrator of ScholarWorks at University of Montana. For more information, please contact scholarworks@mso.umt.edu.

COPYRIGHT ACT OF 1976

THIS IS AN UNPUBLISHED MANUSCRIPT IN WHICH COPYRIGHT SUBSISTS. ANY FURTHER REPRINTING OF ITS CONTENTS MUST BE APPROVED BY THE AUTHOR.

MANSFIELD LIBRARY

UNIVERSITY OF MONTANA

DATE: 1983

KINEMATIC INTERPRETATION OF
MYLONITIC ROCKS IN OKANOGAN DOME,
NORTH-CENTRAL WASHINGTON,
AND IMPLICATIONS FOR DOME EVOLUTION

by

Vicki L. Hansen

B. A., Carleton College, 1980


Presented in partial fulfillment of the
requirements for the degree of

Master of Science

UNIVERSITY OF MONTANA

1983

Approved by:


Chair, Board of Examiners


Dean, Graduate School

5-27-83
Date

UMI Number: EP38243

All rights reserved

INFORMATION TO ALL USERS

The quality of this reproduction is dependent upon the quality of the copy submitted.

In the unlikely event that the author did not send a complete manuscript and there are missing pages, these will be noted. Also, if material had to be removed, a note will indicate the deletion.



UMI EP38243

Published by ProQuest LLC (2013). Copyright in the Dissertation held by the Author.

Microform Edition © ProQuest LLC.

All rights reserved. This work is protected against unauthorized copying under Title 17, United States Code



ProQuest LLC.
789 East Eisenhower Parkway
P.O. Box 1346
Ann Arbor, MI 48106 - 1346

ABSTRACT

Hansen, Vicki L., M. S., May 1983

Geology

Kinematic interpretation of mylonitic rocks of the Okanogan dome, north-central Washington, and implications for dome evolution

Director: Donald W. Hyndman



Mylonitization and later brecciation of granodiorite record the environment and timing of ductile and brittle deformation in the Okanogan dome. Deformation and high-grade metamorphism of sedimentary rocks was accompanied and followed by emplacement of granodiorite plutons. The paragneiss and granodiorite were mylonitized, then warped and domally uplifted with coincident development of joints, dikes, and chloritic breccia.

The mylonite zone dips west to southwestward and is about 1.5 km thick. Mylonitization increases structurally upward within the dome. Quartz, biotite, and plagioclase record a mylonitic foliation (S) containing a unidirectional elongation lineation. Superimposed shear surfaces (C) cut the foliation at an angle of 10-45°, the angle decreasing with increasing mylonitization. The angle of inclination of S to C indicates a sense of westward displacement, of upper plate rocks relative to lower plate rocks, in a direction parallel to mylonitic lineation. This sense of shear is opposite to the shear indicated by quartz c-axes and reoriented folds (Godge, 1983) and stretched inclusions.

The mylonitic fabric formed isochemically under middle-green-schist conditions as determined by plotting the percent Ab component in coexisting recrystallized feldspars.

A zone of intense chloritic breccia disrupts the mylonitic layering along the west and southwest border of the dome. The zone, about 30 m thick, is subparallel to the mylonitic foliation and confined to the dome margin. Clay gouge, slickensides, and polished surfaces are prominent within the breccia zone.

It is conceivable that the Okanogan mylonite zone experienced earlier easterly directed shear as indicated by reoriented folds and stretched inclusions, followed by later westerly directed shear as indicated by the S and C asymmetry. The ductile mylonitic deformation was followed by more-recent movement which caused brecciation of the mylonitic layering.

ACKNOWLEDGEMENTS

I am indebted to Dave Alt, Brain Atwater, Ken Fox, John Goodge, Don Hyndman, Dean Rinehart, and Steve Sheriff for lively discussions in the field and many helpful suggestions. I extend special thanks to John Goodge and Don Hyndman for insights, encouragement, and patience. I accept full responsibility for the (mis)interpretation within this report, and thank Carol Simpson and Gordon Lister for their challenging remarks which opened my mind to the "truth". This work was accomplished with generous support from the U. S. Geological Survey and the Colville Confederate Tribes, and through research grants from the Geological Society of America (2990-02) and Sigma Xi.

TABLE OF CONTENTS

	Page
ABSTRACT	ii
ACKNOWLEDGMENTS	iii
LIST OF FIGURES AND TABLES	v
INTRODUCTION	1
GENERAL GEOLOGY	7
MYLONITIC FABRIC	8
Fabric Interpretation	13
Megacryst Patterns	23
CHEMISTRY	30
Feldspar Mineralogy	32
Biotite Chemistry	35
CONCLUSIONS	40
TECTONIC FRAMEWORK	41
REFERENCES CITED	48

LIST OF FIGURES AND TABLES

Figure	Page
1. Metamorphic core complexes of the North American Cordillera2
2. Location map of the Okanogan dome, north-central Washington2
3. Generalized geologic map of Omak Lake 15' quadrangle	4
4. Biotite schistose inclusion in megacrystic granodiorite . . .	10
5. Block diagram of mesoscopic mylonitic fabrics	10
6. Photomicrographs of mylonitic textures	15
7. Generalized sketch of Mm and Mc	21
8. Block diagram of microscopic mylonitic fabrics	21
9. Sketch of Mc and Mm with interpreted shear24
10. Models of feldspar megacryst deformation24
11. Model of feldspar megacryst rotation24
12. Comparision of Mm and Mc with literature28
13. Comparision of Mm and Mc with S and C	28
14. Comparision of Mm and Mc with Sc and Sm	28
15. Ternary diagram of feldspar Ab, An and Or components34
16. Graph of percent Ab in coexisting recrystallized feldspar . . .	34
17. Ternary disgram of Fe, Mg and Ti in Mc and Mm biotite	37

TABLE

I. Rotation of feldspar megacrysts	37
II. Whole rock major element analyses	38
III. Plagioclase mineralogy and chemistry	38
IV. Orthoclase mineralogy and chemistry	38
V. Coexisting feldspars	39
VI. Biotite mineralogy and chemistry	39

ADDENDUM

In the following report I present a logical argument for a top-to-the-east sense of shear during the formation of the Okanogan dome mylonitic zone, north-central Washington. Although the argument appears logical and internally consistent, it is based on the assumption that the major shear plane parallels the mylonitic foliation (Mc), marked by compositional layering (page 27). If Mc, as I describe it, formed by stretching RATHER THAN by major shear, my interpretation of the mylonitic fabrics is incorrect. Mm planes would then describe the major sense of shear during formation of the mylonite zone, and hence the shear described by the asymmetry of the Mc and Mm planes if top-to-the-west.

Based on the orientation of quartz subgrains this reinterpreted top-to-the-west sense of shear appears correct. Elongate quartz subgrains, interpreted as qualitative strain ellipsoids, are tilted to the west and inclined at an acute angle to Mm. Mm planes then become the interpreted planes of shear which deformed the resultant quartz subgrains (Fig. A). The shear on Mm planes is left lateral, or top-to-the-west, in a direction parallel to mylonitic lineation. Given this revised interpretation my Mc planes correspond to S planes mylonitic schistosity, of Berthe et al (1979), and my Mm planes correspond to C planes, shear planes, of Berthe et al (1979). Read cautiously and critically dear reader--my argument sounds logical and internally consistent.

Unfortunately/fortunately the Okanogan story is not yet as simple as top-to-the-east versus top-to-the-west. Although the petrotectures of the megacrystic granodiorite seem to now be telling us top-to-the-west, stretched inclusions (Fig. 4), and reoriented metamorphic folds and quartz c-axes (Goodge, 1983) describe a top-to-the-east sense of shear within the mylonite zone. It may be that the Okanogan mylonitic formed during earlier easterly directed shear as described by macroscopic inclusions and reoriented folds, and later experienced westward directed shear reflected on a smaller scale in the Mc-Mm asymmetry...but why then the easterly biased quartz c-axes? As any good study this research asks more questions than it answers.

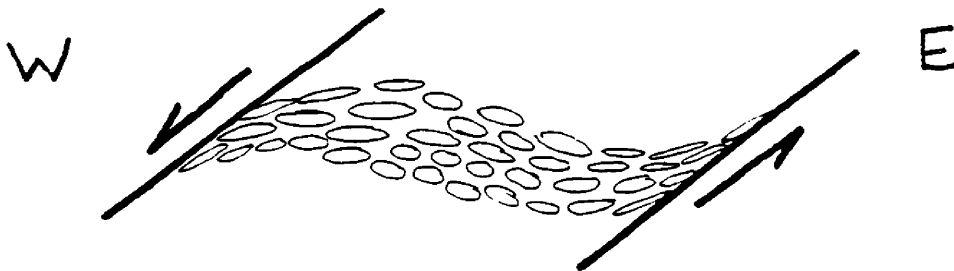


Fig. A

INTRODUCTION

Okanogan, Kettle, and Spokane domes in northeastern Washington extend south from the Shuswap metamorphic complex of south-central British Columbia (Fox et al, 1977; Cheney, 1980; Rhodes and Cheney, 1981). These crystalline domes along with at least 22 others form a sinuous chain along the North American Cordillera from southern Canada to northwestern Mexico (Fig. 1) (Davis and Coney, 1979). They have attracted considerable attention as metamorphic core complexes (see Crittenden et al, 1980). The salient features of Cordilleran metamorphic core complexes include a high-grade metamorphic-plutonic infrastructure deformed by a gently-dipping mylonite zone overprinted by a zone of chloritic breccia. Above the breccia zone suprastructural rocks are metamorphosed as high as sillimanite zone of the amphibolite facies although greenschist-grade is most common. The role of the mylonitic deformation in dome genesis remains controversial. In this paper I describe the mylonitic rocks and their textures, and conclude that their fabric formed isochemically under middle-greenschist facies conditions as rocks above the mylonite zone were displaced eastward relative to dome rocks. This conclusion is based on the percent albite component in coexisting recrystallized feldspars (Stormer, 1975) and an interpretation of textural asymmetry within the mylonitic fabric similar to that of Berthe et al (1979).

Okanogan dome consists of 2,500 square kilometers of metasedimentary

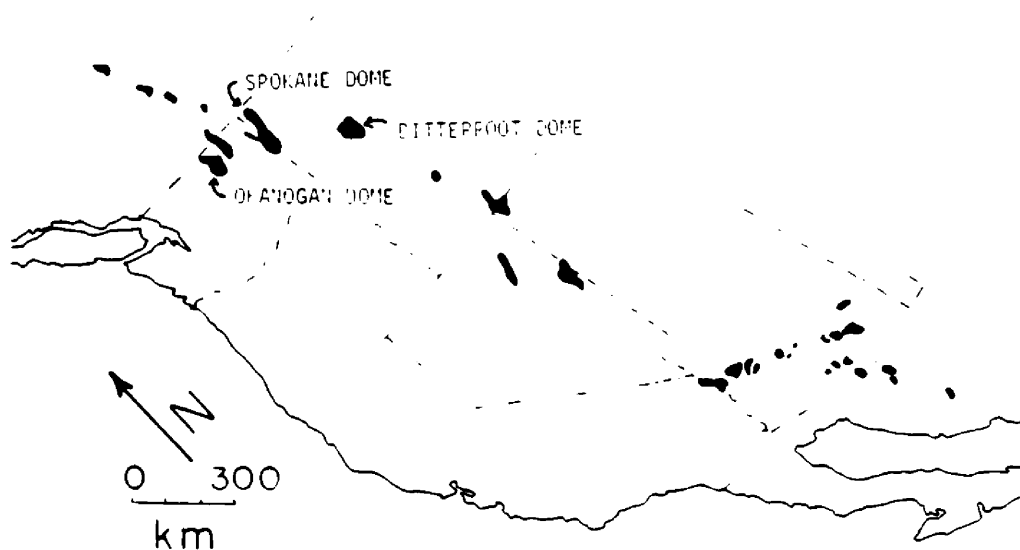


FIG. 1. Location of metamorphic core complexes along the North American Cordillera from Canada to Mexico (adapted from Davis and Coney, 1979).

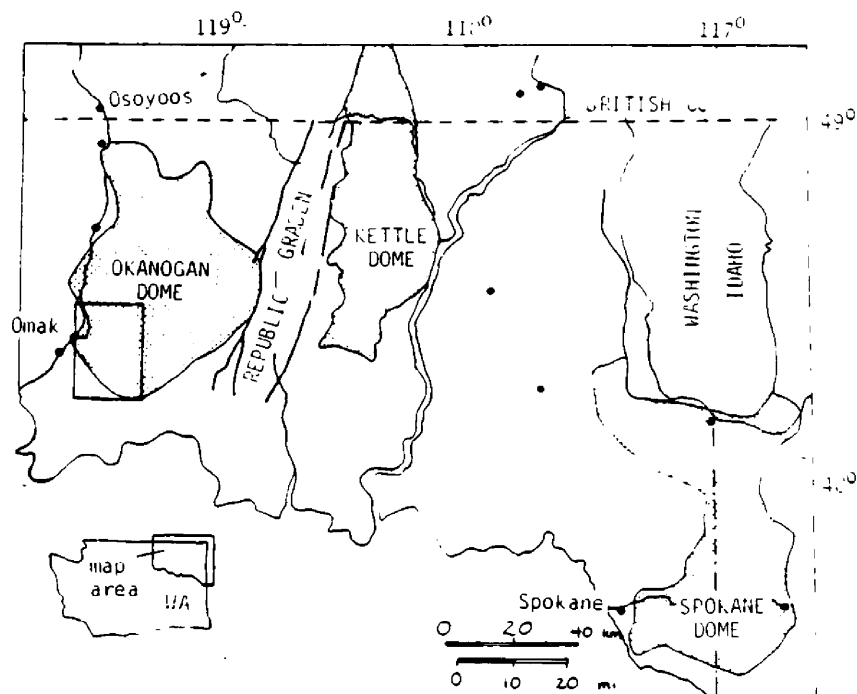


FIG. 2. Location map of the Okanogan dome, northeastern Washington. Omak Lake 15' quadrangle is shown in the southwest portion of Okanogan dome. (Adapted from Cheney, 1980).

gneiss and massive granitoid gneiss cut by Eocene age granitic plutons (Fox et al, 1976). Okanogon dome is separated from Kettle dome to the east by Tertiary volcanic rocks and clastic terrigenous sedimentary rocks of the Republic Graben; rocks of Okanogon dome are nearly continuous to the north with high-grade rocks of the Shuswap metamorphic complex (Fig. 2). Tertiary basalts of the Columbia Plateau end abruptly at the southwest dome boundary (Fig. 3). Rocks within the dome record Eocene K-Ar ages (Fox and Rinehart, 1971). Low-grade metamorphosed sedimentary rocks of Triassic age or older, flank the dome to the north and northwest (Fox et al, 1971, 1976, 1977). High-grade paragneiss and associated plutonic rocks flank the dome to the south and southwest (Goodge and Hansen, in press; B. Atwater, pers. comm.). Okanogon dome, forming the western-most boundary of the Omineca crystalline belt (Fox et al, 1976), is bounded to the west by the Okanogon fault and to the south by the Omak Lake fault (Snook, 1965; Goodge and Hansen, in press). An extensive, well-developed mylonite zone, up to 1.5 km thick, penetrates rocks of the crystalline core along the northern, western, and southern borders of the dome (Waters and Krauskopf, 1941; Snook, 1965). The mylonitic fabric, consisting of a foliation and unidirectional lineation, dies out in the dome interior (Fig. 3). A randomly fractured breccia cuts the mylonitic fabric along the western and southern dome boundaries (Waters and Krauskopf, 1941; Snook, 1965; McMillen, 1981; Hansen, 1983, Goodge and Hansen, in press).

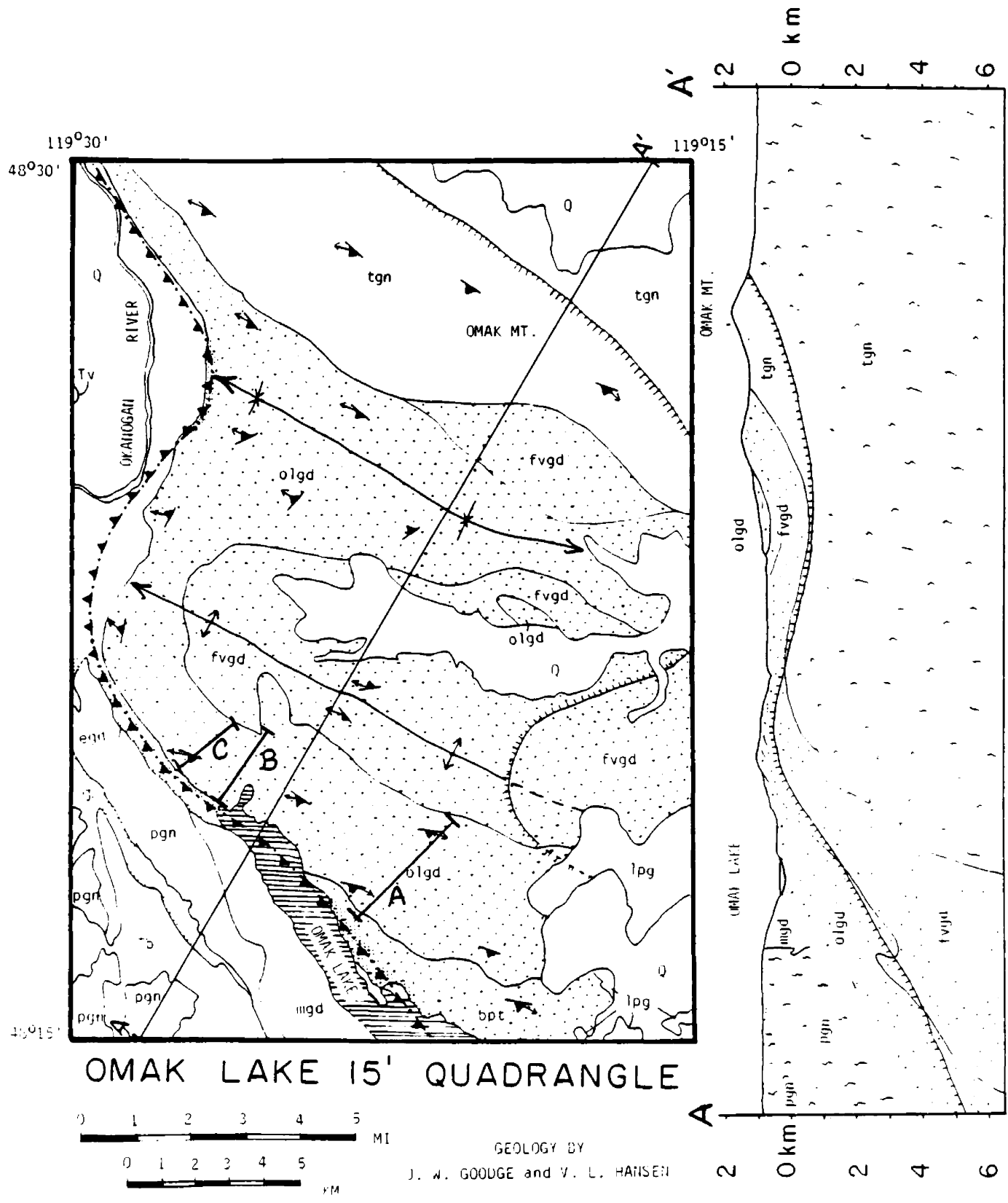


FIG. 3. Generalized geologic map of the Omak Lake 15' quadrangle, Okanogan County, Washington.

MAP SYMBOLS



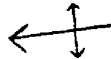
lithologic contacts



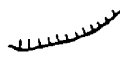
chloritic breccia zone



synform showing trace of axial plane and plunge of axis



antiform, showing trace of axial plane and plunge of axis



limit of mylonitic deformation; mylonitized rock on hatched side of line-gradational boundary



strike and dip of mylonitic foliation



trend of mylonitic lineation

Q

Quaternary Deposits

Tb

Columbia River Basalt

Tv

Coleman Butte volcanics

lpg

Luocratic porphyritic granite
White to grey, medium- to coarse-grained porphyritic granite. Contains pegmatite and aplite dikes. Weak mylonitic fabric occurs locally along south end of Omak Lake. lpg intrudes bpt along the southeastern margin of Omak Lake.

fvgd

French Valley biotite granodiorite
Light-grey, medium-grained, equigranular biotite granodiorite with minor hornblende, sphene, apatite, and Fe oxide. Contacts with olgd gradational over 50 m but probable xenoliths of olgd suggest fvgd is younger.

olgd

Omak Lake K-feldspar megacryst biotite granodiorite
Light to medium-grey biotite granodiorite contains up to 5% K-feldspar megacrysts. Equigranular matrix contains quartz, plagioclase, biotite and minor sphene and Fe oxide. Unit is cut by pegmatite and aplite dikes and contains tabular to rounded inclusions of amphibolite and biotite schist.

bpt

Bull Pasture hornblende-biotite tonalite
Dark grey to black, medium-grained, equigranular, locally layered, spotted tonalite. Unit is intruded by olgd and lpg.

egd

Equigranular (hornblende-) biotite granodiorite
Light-grey, medium-grained, massive, equigranular granodiorite contains minor hornblende, sphene, apatite, epidote and chlorite. Cl, hornblende: biotite ratio and sphene content commonly increase near contact with pgn. Contact zone is 0.5 km wide, becoming wispy to migmatitic.

mgd

K-feldspar megacryst biotite granodiorite
Coarse-grained, massive to foliated, blue-grey rock contains K-feldspar megacryst (1-6cm). Flow foliation parallels mafic inclusions. Unit is cut by alaskite, and aplite and pegmatite dikes.

tgn

Tonasket Gneiss (usage after Fox et al, 1976)
Undivided assemblage of high-grade gneisses including hornblende-biotite gneiss, biotite gneiss, augen gneiss, sillimanite-garnet-muscovite-biotite schist, biotite quartzite, amphibolite, diopside calc-silicate gneiss, and garnet alaskite gneiss. Unit is intruded by olgd and fvgd to the south.

pgn

Paragneiss
Undivided assemblage of high-grade, compositionally layered gneisses including hornblende-biotite gneiss, augen gneiss, biotite gneiss, sillimanite-muscovite-biotite schist, biotite-quartzofeldspathic gneiss, amphibolite, quartzite, biotite quartzite, marble, garnet-pyroxene calc-silicate gneiss, coarse hornblendite, and minor metamorphic (?) dunite. Unit is intruded by mgd and egd.

Geologic relations observed along the southwest border of Okanogan dome constrain several models presented by earlier workers attempting to explain the origin of the rocks and their structures. Waters and Krauskopf (1941) originally attributed both the mylonitic and cataclastic textures to protoclasic emplacement of the "Colville batholith" defined by Pardee (1918) (see Fox et al, 1976, p. 217-219). Snook (1965) reexamined western and southwestern sectors of the dome and concluded that parent rocks of the core gneiss, the Tonasket gneiss, are sedimentary and volcanic rocks regionally metamorphosed to high-grades. According to Snook the gneiss was subsequently cut by a deep-seated, low-angle thrust fault which produced a mylonitic fabric. The area was then raised along the Okanogan Valley and Omak Lake faults causing brecciation and retrograde chloritization. These normal faults placed low-grade metamorphic rocks against high-grade core gneiss to the east. Snook's interpretation accounts for the unidirectional mylonitic lineation, and the very different environments during formation of mylonite and breccia.

Fox et al (1971, 1976, 1977) studied the area further; they identified and redefined a centrally located body of paragneiss, the Tonasket gneiss, and a discontinuous peripheral body of gneissic to massive granitoid rocks. These workers disclaim Snook's late-stage normal faults and attribute the penetrative deformation and metamorphism of dome rocks to mobilization and diapiric intrusion of core rocks into low-grade country rocks. Fox et al, like Waters and Krauskopf, attribute both the mylonite and breccia to diapiric

emplacement of a crystalline core. Cheney (1980) suggests that thrusting and cataclasis separated a basement of Precambrian metamorphic rocks and Mesozoic to Tertiary plutons from Precambrian and Tertiary layered rocks. Folding and doming followed during Eocene time.

This paper discusses the southwest border of the Okanogan dome, and stems from geologic mapping in the Omak Lake 15' quadrangle (Fig. 3). My research involves field mapping and laboratory study, including analysis of microscopic fabrics and microprobe study of samples collected in three traverses through the mylonite zone. The objective is to constrain models of mylonite formation, and hence dome evolution.

GENERAL GEOLOGY

Within the Omak Lake 15' quadrangle, Okanogan dome is bounded to the west by the Okanogan fault, and to the south by the Omak Lake fault (Snook, 1965). An extensive and well-developed mylonite zone, up to 1.5 km thick, penetrates the dome rocks along the northern, western and southern borders of the dome, and is overprinted by a narrow zone of chloritic brecciation along the southwest border within the study area. Rocks outside the southwest margin are divided into four groups: high-grade layered metasedimentary gneiss, felsic granitoid rocks, mafic to felsic dikes, and Tertiary basalt. Rocks within the southwest portion of the dome also comprise four major lithologic units: high-grade layered metasedimentary gneiss, homogeneous

orthogneiss, leucocratic porphyritic granite, and microdiorite dikes. All units inside the dome, with the exception of microdiorite, are deformed by varying degrees in the mylonite zone. Pre-mylonite geologic histories of rocks inside and outside Okanogan dome are strikingly similar. Both packages of rock record deposition of eugeoclinal sediments followed by high-grade regional metamorphism and deformation to form paragneiss sequences displaying strong metamorphic textures. Folding occurred during or after the peak of regional metamorphism. A sequence of granodiorite to tonalite plutons intruded the paragneiss assemblages, followed in turn by intrusion of leucogranite. At this point the geologic histories of these two rock packages diverge. The rocks of Okanogan dome were deformed by penetrative, unidirectional mylonitization, followed by more restricted chloritic brecciation along its borders. Rocks west of the dome margin are not mylonitized, yet they record brecciation and chloritization similar to brittle deformation along the dome margin. A deformation which accompanied and followed mylonitization warped the mylonite zone into gently plunging, megascopic, antiforms and synforms. North-east-trending vertical joints formed in the dome and microdiorite dikes subsequently intruded along these joint planes (see Goodge and Hansen, in press).

MYLONITIC FABRIC

My research focuses on mylonitized megacrystic granodiorite in order to determine the environment of mylonite formation. Orthogneisses,

exposed in a broad band northeast of Omak Lake, cover the greatest portion of the study area (Fig. 3). Three major compositional phases are recognized, K-feldspar-megacryst biotite granodiorite, equigranular biotite granodiorite and hornblende-biotite tonalite, all of which contain numerous pegmatite and aplite dikes, and amphibolite and biotite-schist inclusions. Megacrystic granodiorite (olgd) is a light- to medium-gray-colored (CI = 5-7), homogeneous-textured plutonic rock containing conspicuous pink or grey K-feldspar megacrysts (2-8 long cm) comprising 1 to 5 percent of rock volume. Its matrix is medium-grained (0.5-5.0 mm) and equigranular, and contains quartz, plagioclase, biotite, and minor orthoclase, sphene, allanite, and opaque Fe-oxide. Megacrystic granodiorite is in sharp contact (~10 m wide) with tonalite and equigranular granodiorite. However, the three units are probably contemporaneous phases of a single pluton as indicated by xenocrysts of K-feldspar megacryst in equigranular granodiorite and tonalite near their contacts with megacrystic granodiorite, inclusions of megacrystic granodiorite in equigranular granodiorite, and wide dikes of megacrystic granodiorite cutting equigranular granodiorite.

Dominating the form and structural fabric of the rocks within Okanogan dome is a penetrative zone of mylonite, as defined by Bell and Etheridge (1973). This broad zone conforms to the dome perimeter, and forms "flat-iron"-like aprons slanting up eastward from the Okanogan Valley as well as the gentle domal shape of the Okanogan highlands. The mylonite ranges in thickness from 1.0 to 1.5 km, and intensity

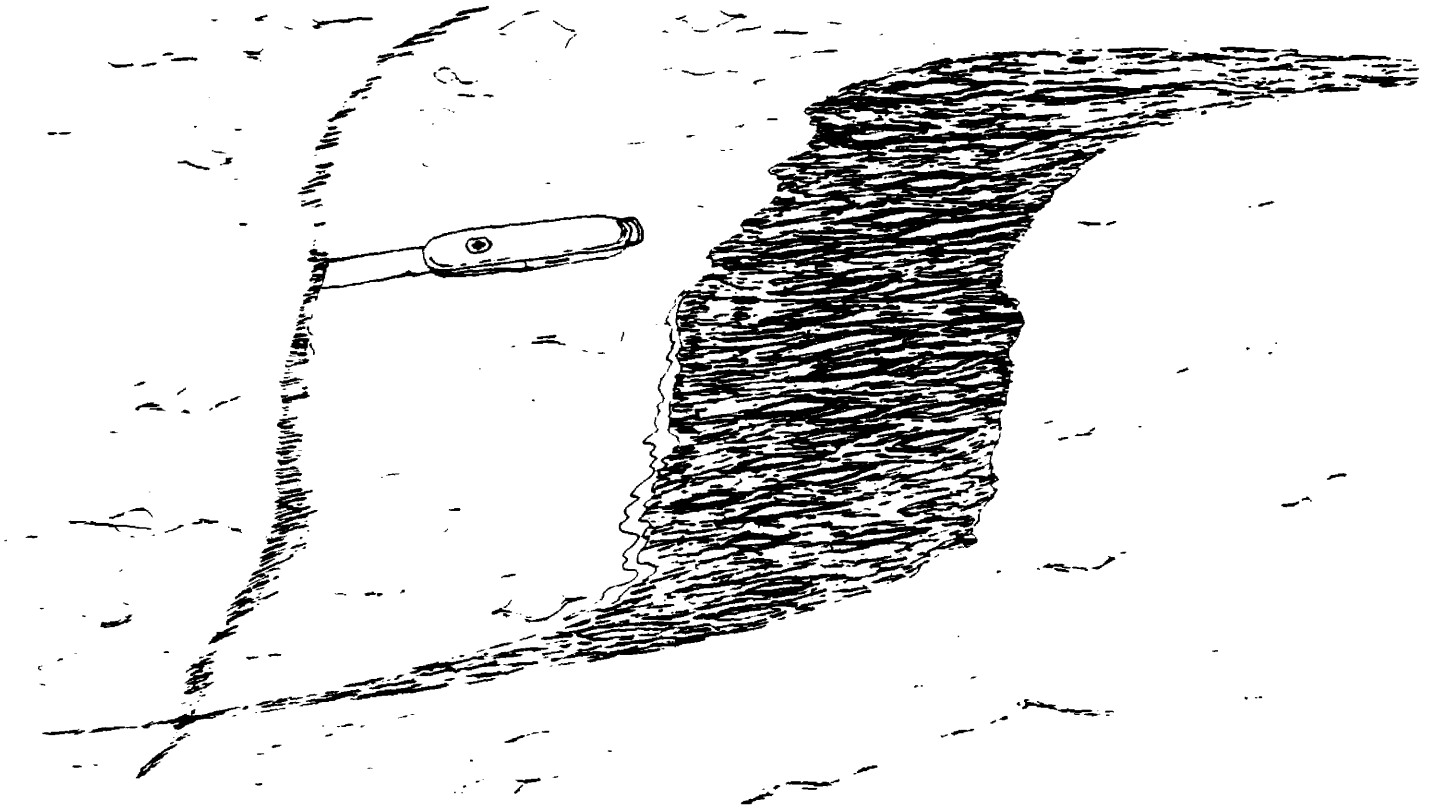


FIG. 4. Biotite schistose inclusion in megacrystic granodiorite; inclusion is viewed northward in a plane parallel to mylonitic lineation and normal to mylonitic foliation.

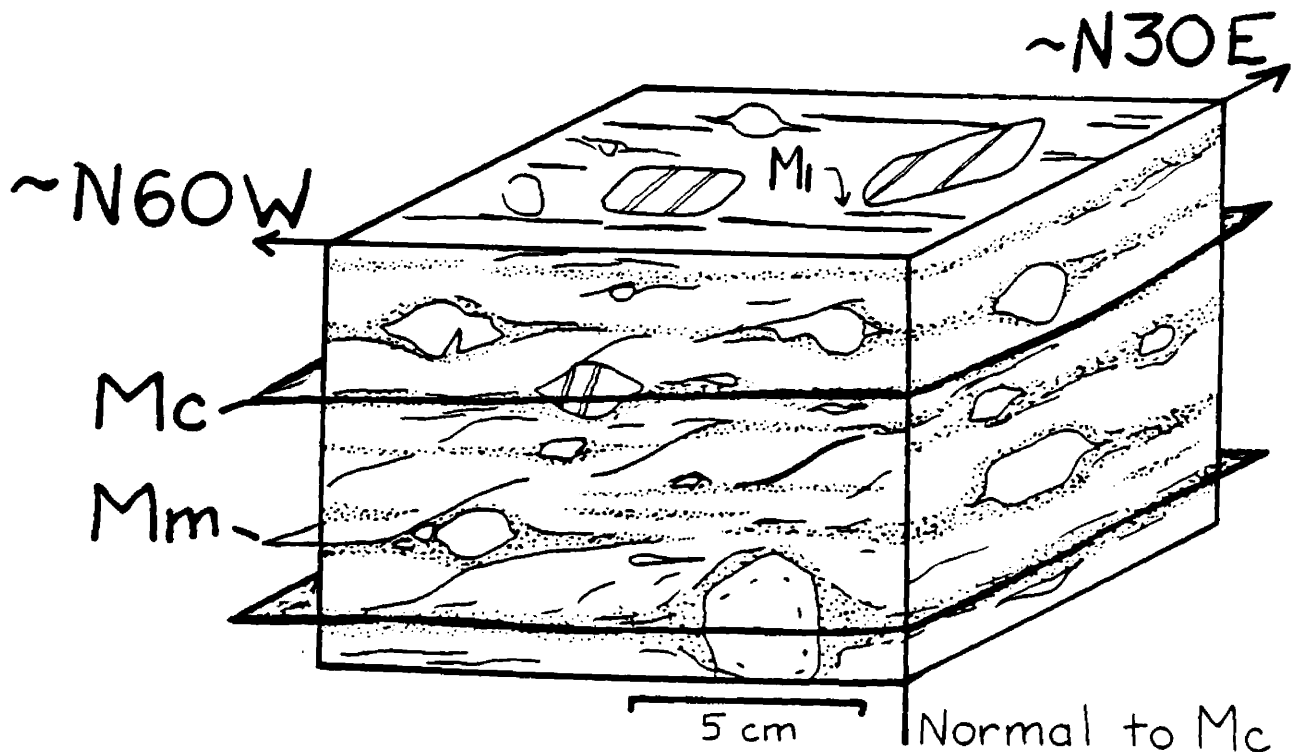


FIG. 5. Block diagram of mesoscopic mylonitic fabrics. Note that sections cut normal to M_c and parallel to M_l are viewed northward, and sections cut normal to both M_c and M_l are viewed westward.

of deformation increases upward in the dome. Mylonitic deformation increases toward the western and southern dome boundaries. It is well defined in the orthogneiss near border areas of Okanogan dome. The mylonitic foliation is a broadly planar biotite and quartz fabric, which on a grain scale is wavy or sigmoidal in coarse-grained orthogneiss. In the mylonitic foliation plane, elongate lenses and streaks of aggregate biotite, quartz and plagioclase define a unidirectional lineation. Strikes of the mylonitic foliation grossly parallel the dome boundary, but lineation bearings fall consistently in the ranges 140° - 155° .

Three mesoscopic features of the mylonitic structures indicate important aspects of the physical conditions during deformation; 1) relative orientations of pegmatite dikes within the zone, 2) deformed inclusions, and 3) pull-apart fractures in K-feldspar-megacrysts. Planes of numerous pegmatites and mafic dikes which intrude K-feldspar megacryst granodiorite show increased concordance to mylonitic foliation upward in the mylonite zone. This pattern is a consequence of increased deformation toward higher structural levels in Okanogan dome, and reflects not only greater shear strain but greater overall tectonic transport toward the margin of the dome. Biotite-rich schistose inclusions are elongate with an upper tail stretched eastward and a lower tail westward, as viewed on a plane normal to mylonitic foliation and parallel to mylonitic lineation (Fig. 4). The pattern of these inclusions suggests dextral shear in the mylonite zone, viewed northward. In K-feldspar megacryst granodiorite,

megacrysts are cut by planar brittle fractures oriented perpendicular to mylonitic lineation. The fractures end abruptly at crystal boundaries, do not cut into mylonitic foliation, appear unrelated to crystal orientation, and commonly contain a quartz-chlorite-epidote mineral assemblage. Formation of the fractures must be a response to mylonitization and not a post-mylonitic period of brittle deformation, because they cut only megacrysts, not the mylonitic fabric. Such pull-apart fractures also indicate that mylonitization involved local extensional strain.

To determine the environment of mylonite formation, I collected rock samples at seven or more stations along each of three traverses through progressively mylonitized homogeneous megacrystic granodiorite, and studied trends in mineral and chemical composition, and textures (Fig. 3). I collected oriented samples for thin section and microprobe mounts at every station along each traverse, and samples for whole-rock chemical analysis and specific gravity at every other station along each traverse. Sections for petrofabric and microprobe analysis are consistently oriented with mylonitic foliation and lineation as depicted in Figure 5. Sections cut normal to mylonitic foliation, Mc, and parallel to mylonitic lineation, Ml, are viewed northward; sections cut normal to Mc and Ml, are viewed westward. Sections from traverse A were used for microprobe analysis.

FABRIC INTERPRETATION

Mylonitic deformation of megacrystic granodiorite produced an asymmetric penetrative fabric consisting of several mesoscopic and microscopic fabric elements. The most striking mesoscopic fabric is mylonitic foliation and lineation. Layers or lenses rich in quartz interspersed with layers of biotite and feldspar define a well-developed planar compositional mylonitic foliation, Mc. Within the foliation plane, streaks of biotite, quartz, and plagioclase define a unidirectional mylonitic lineation, M1. In the Omak Lake 15' quadrangle, this lineation trends approximately 150°. Blocky elongate K-feldspar megacrysts commonly display quartz-filled, sub-vertical fractures oriented normal to M1 (Fig. 5). In sections cut normal to Mc and parallel to M1, a weakly- to moderately-developed crenulation cleavage, Mm, crosses the mylonitic foliation, defining a fabric asymmetry. The crenulation cleavage, Mm, is variably developed, striking parallel to mylonitic foliation, Mc, and dips more steeply westward 15-45° (Fig. 5). The intersection of these two planes is normal to M1. Aligned and smeared biotite grains coat the Mm plane defining its role as a slip surface. These biotite grains mark a second lineation, M2, within the plane of Mm nearly parallel to M1, though plunging more steeply westward. On surfaces cut normal to both Mc and M1, a single planar foliation continuous with Mc is present. Mm is best developed high in the structural section where the mylonitic fabric is strongest. In the field, Mc is the dominant foliation; Mc is planar and continuous whereas Mm resembles

chattermarks or unidirectional scalloped surfaces 1 to 2 cm across cutting Mc surfaces at a consistent angle. The planar continuity of Mc, and accompanying strong lineation M1, suggest that Mc and M1 are the plane and direction of major tectonic transport.

Similar fabrics and relationships appear in thin section. Layers of alternating quartz and feldspar lenses define mylonitic foliation, Mc, most obviously in plane light. In sections normal to Mc, and parallel to M1, quartz lenses form sigmoidal layers which thicken and thin asymmetrically between planar enveloping surfaces parallel to mesoscopic Mc (Fig. 6.a). Elongate quartz subgrains observed in polarized light show aspect ratios of 4:1 to 10:1 roughly parallel to the outline of the sigmoidal quartz lenses. Greater ratios structurally high in the mylonite zone reflect increased mylonitic deformation.

In sections normal to Mc and parallel to M1, slip surfaces Mm intersect Mc at positions along the thinned limbs of quartz in Mc (Figs. 6.b and 7). Mm surfaces are marked by biotite and other mafic minerals, and zones of ductile grain-size reduction of feldspar and stretching or elongation of quartz (Figs. 6.b and 6.c). Biotite forms stringers of short, very fine-grained (35 μ m) biotite film along Mm planes. The angular intersection of Mc and Mm defines a textural asymmetry in sections parallel to M1 and a symmetrical planar foliation in sections parallel to the Mc-Mm intersection lineation in sections normal to M1 (Fig. 8). The significance of Mc and Mm asymmetry observed in sections normal to Mc and parallel to M1, is discussed below.

Fig. 6.a. Layers of alternating quartz and feldspar lenses define mylonitic foliation, Mc, best seen in plane light. Section is cut normal to Mc and parallel to M1; field of view is 8.5 mm.

Fig. 6.b. In sections normal to Mc and parallel to M1, slip surfaces Mm intersect horizontal Mc at an acute angle. Mm surfaces are marked by biotite and other mafics, and zones of ductile grain-size reduction of feldspar and elongation of quartz.

Fig. 6.d. Mm rarely truncates Mc totally; rather it deflects Mc reflecting minor shear along Mm. Feldspar megacryst offset along Mm shows measurable left-lateral displacement viewed northward. Field of view is 3.5 mm.

Fig. 6.e. Mm planes owe their short length to truncation by movement along Mc planes as evidenced by biotite in this photomicrograph which is 3.5 mm across. The fine-grained biotite stringer marking Mm is rotated into Mc indicating right-lateral movement along Mc.

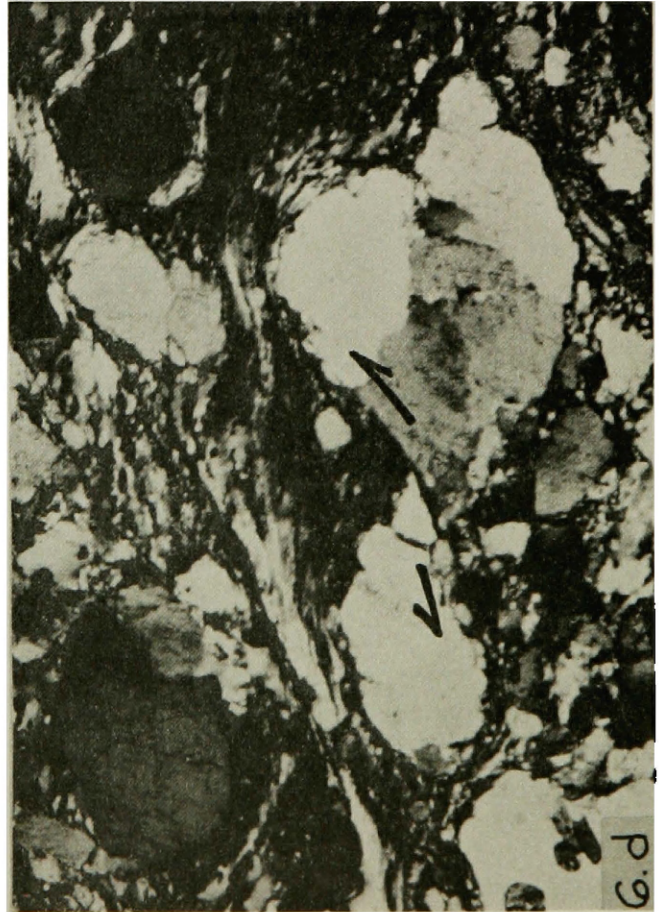
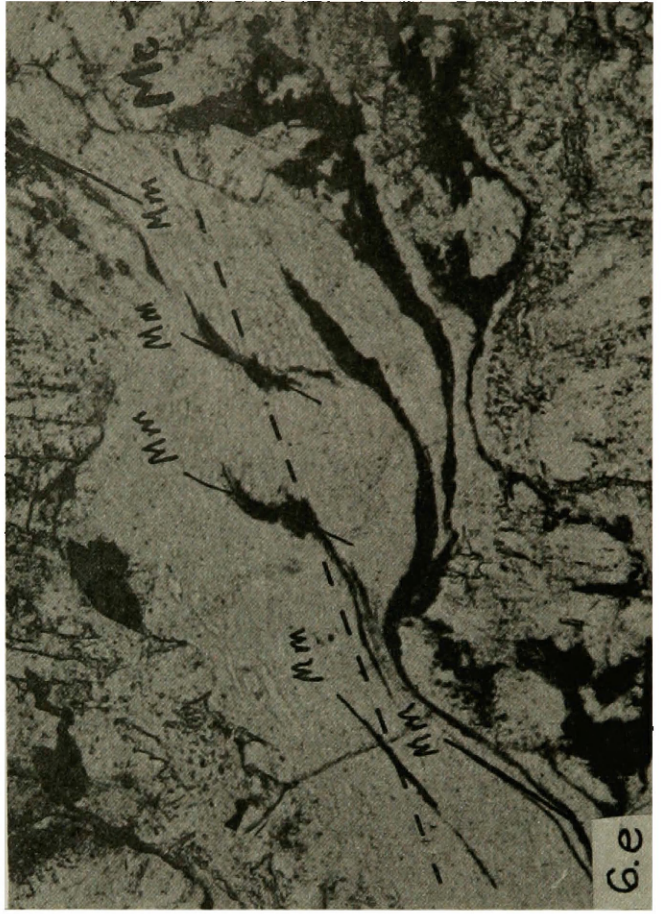
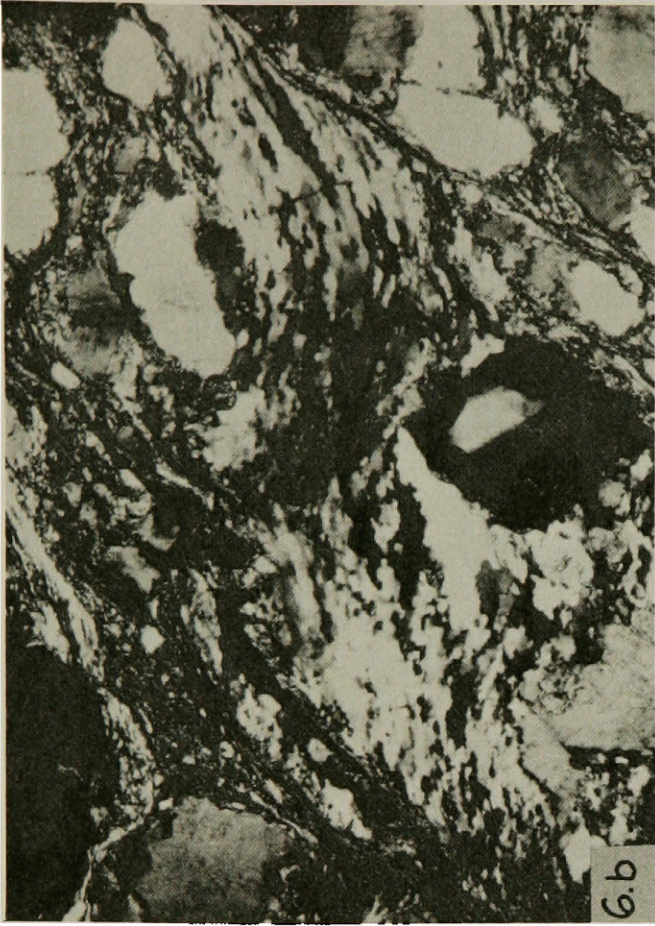


Fig. 6.c. The angular intersection of Mc and Mm define a textural asymmetry in sections parallel to M1. Mc is horizontal with Mm cutting at an angle of 30° . Note the sigmoidal nature of Mc; the enveloping surface of microscopic Mc parallels mesoscopic Mc. Field of view is 8.5 mm.

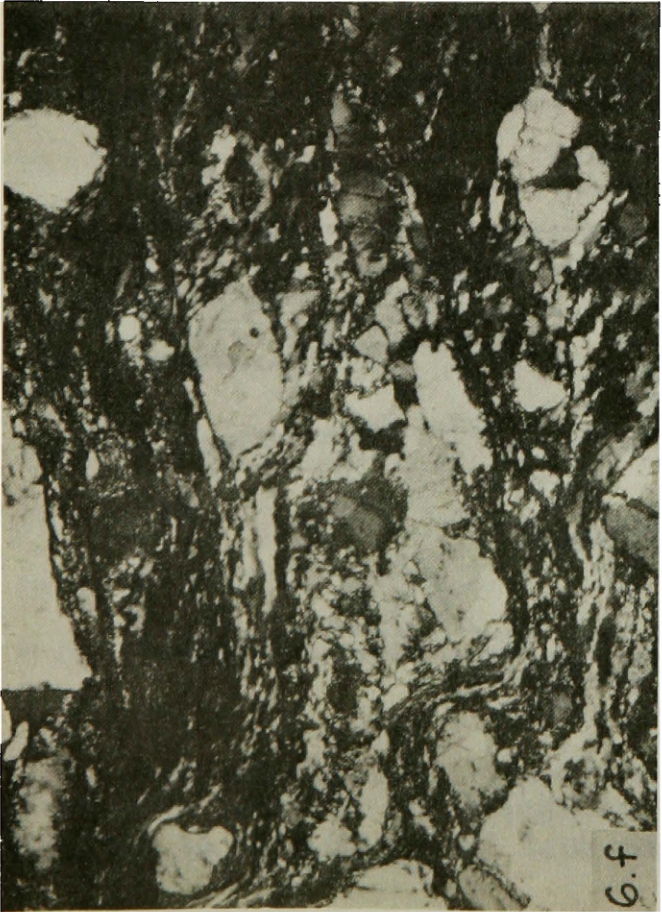
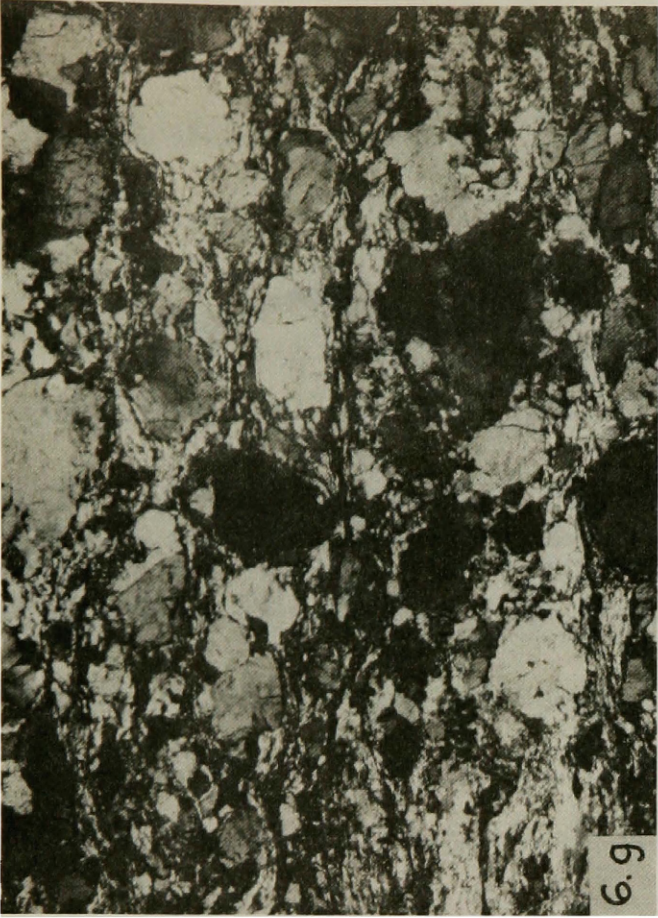


Fig. 6.f. In sections parallel to M1, megacrysts display imbrication, tilted eastward relative to Mc which is horizontal. Field of view is 3.5 mm.

Fig. 6.g. In sections cut normal to both Mc and M1 no textural asymmetry is developed. Megacrysts are generally rounded and show no preferred orientation, or they are elongate parallel to horizontal Mc and show no imbrication. Field of view is 8.5 mm.

Fig. 6.h. In this photomicrograph, 3.5 mm across, each successive feldspar fragment shows left-lateral offset parallel to Mm. Mc is horizontal.

Fig. 6.i. This fractured feldspar megacryst indicates overall clockwise rotation denoted by the arrows. Mc is horizontal with Mm dipping 30° to the left. Field of view is 8.5 mm.



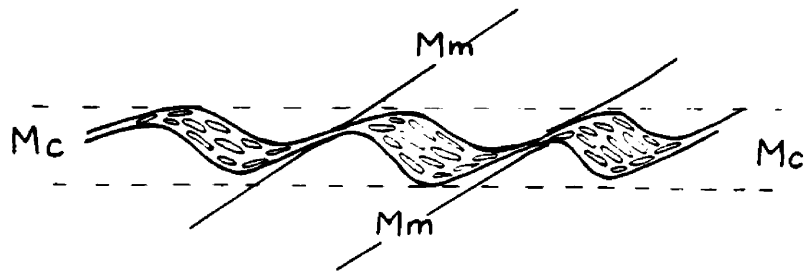


FIG. 7. A generalized sketch of microscopic fabrics show Mm intersecting Mc at positions along the thinned limbs of quartz in Mc. Section is cut normal to Mc and parallel to M1. The planar enveloping surface parallels Mc in hand specimen.

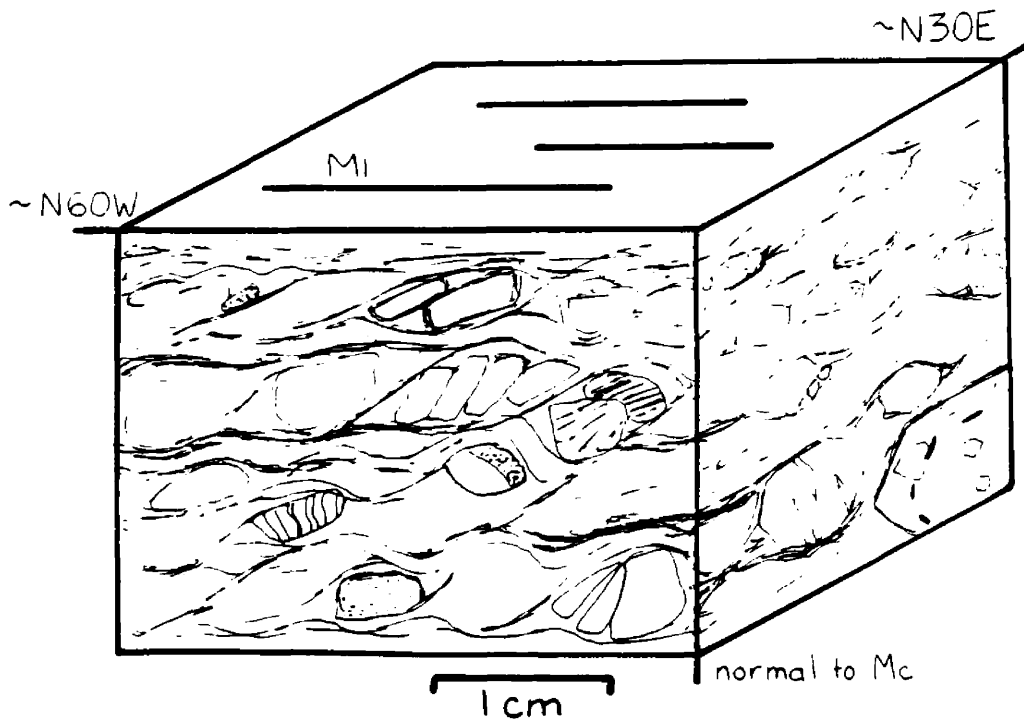


FIG. 8. Intersection of Mc and Mm results in imbrication and fabric asymmetry in sections cut normal to Mc and parallel to M1. Sections cut normal to both Mc and M1 lack imbrication and fabric asymmetry.

Mm planes cross Mc planes along the thinned quartz limbs of Mc. Elongate quartz subgrains of Mc are deformed along Mm planes indicating left-lateral offset as shown in Figure 6.b). Mm rarely truncates Mc totally; rather it deflects Mc reflecting minor shear along Mm. Feldspar megacrysts offset along Mm also show similar small, measurable left-lateral displacement viewed northward (Fig. 6.d). Therefore, mesoscopic smeared-biotite lineation and offset microstructures indicate Mm planes are shear surfaces with slip normal to the Mc-Mm intersection. Mm surfaces show consistent left-lateral offset viewed northward in sections parallel to M1 throughout the studied structural thickness of the mylonite zone.

Although Mm planes deform Mc, Mm planes are short and discontinuous relative to Mc. Mm planes owe their short length to truncation by movement along Mc planes as evidenced by the biotite in Figure 6.3. In this photomicrograph the fine-grained biotite stringer marking Mm is rotated into Mc indicating right lateral movement along Mc. This relationship is typical of Mc-Mm-plane interaction. Whereas Mm planes offset or deflect Mc planes, Mm planes also shallow or merge with Mc planes with the geometry of listric normal faults. In summary, both Mc and Mm planes were loci of shear, or movement. Microstructural evidence indicates that at least a portion of the movement histories overlapped in time with relative apparent offset on each surface pictured in Figure 9; viewed north in sections parallel to M1, Mc and Mm planes indicate right-lateral and left-lateral displacement respectively. A kinematic interpretation of the interaction of Mc and

Mm surfaces is discussed below following the discussion of megacryst geometry.

MEGACRYST PATTERNS

Feldspar megacrysts deflect the planar Mc and Mm surfaces. Megacrysts show kinking, bending, fracturing, and breakage indicative of dominantly brittle deformational processes and the rigid nature of feldspar in a ductile matrix (Lister and Price, 1978; Watt and Williams, 1979). In sections parallel to M1, megacrysts display imbrication, tilted eastward relative to Mc (Figs. 5 and 6.f). This megacryst imbrication is an additional component of the textural asymmetry in the mylonitic fabric. In sections normal to Mc and M1 megacrysts appear generally rounded and show no preferred orientation, or they are elongate parallel to Mc and show no imbrication (Figs. 5 and 6.g).

The imbricate nature of the feldspar megacrysts is portrayed in Figure 6.h. Note the apparent left-lateral offset between several successive feldspar fragments. The resulting domino-like geometry can result through two different movement models (Fig. 10). In the first model (Fig. 10.a) a feldspar megacryst experiences left-lateral simple shear displacement along fractured surfaces parallel to the shear direction. In the second model (Fig. 10.b) the feldspar also experiences left-lateral simple shear displacement along the fractured surfaces. However, this movement is a result of rigid body rotation accompanied by right-lateral shear and resulting overall top-to-the-right

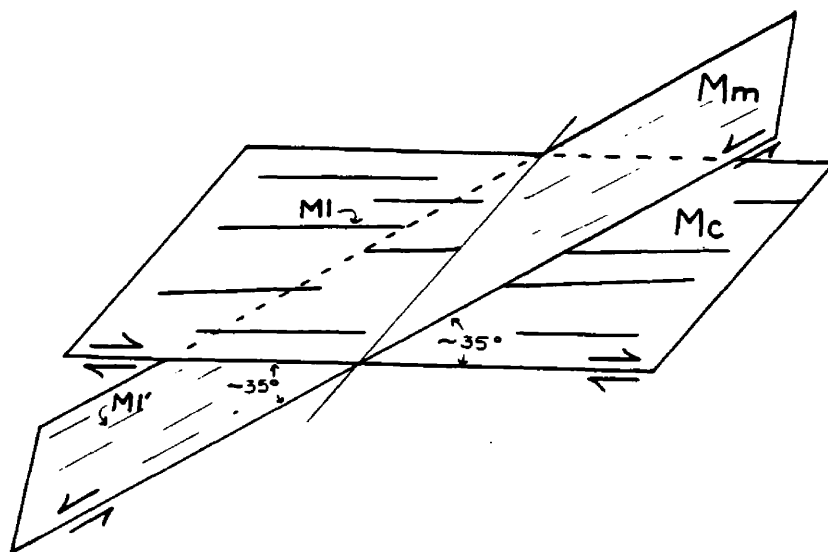


FIG. 9. M_c and M_m planes indicate right-lateral and left-lateral displacement respectively in sections cut normal to M_c and parallel to M_l , viewed northward.

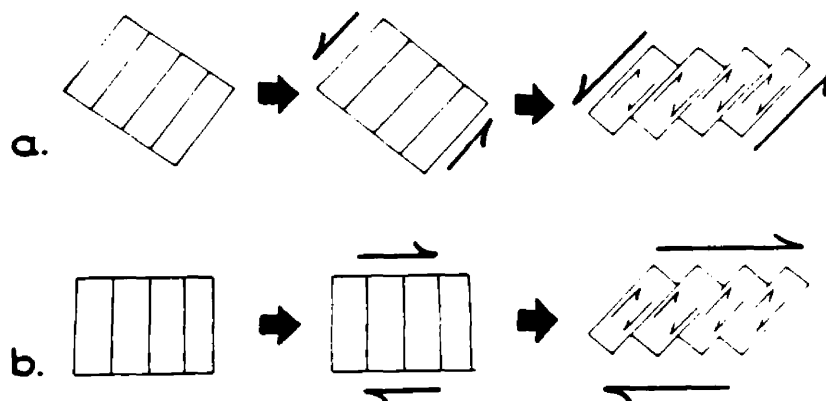


FIG. 10. (a) Feldspar megacryst experiences left-lateral simple shear along fractured surfaces parallel to the shear direction. (b) Feldspar experiences left-lateral simple shear as a result of rigid body rotation accompanied by right-lateral shear resulting in overall top-to-the-right displacement in a horizontal zone.

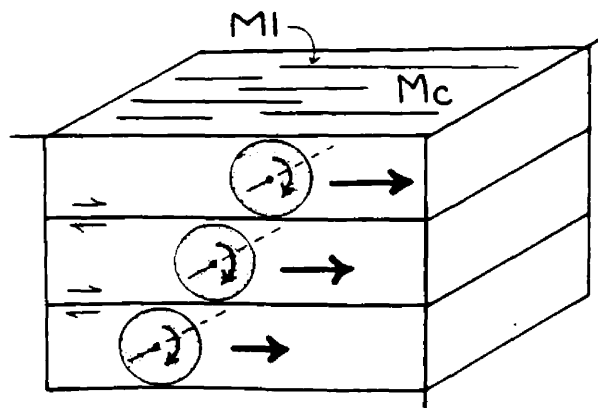


FIG. 11. Rotation of feldspars on axes normal to M_l requires that shear, or tectonic transport, parallel M_l . Clockwise rotation, viewed northward, of these rigid megacrysts indicates right-lateral shear (modified from Beck, 1980).

displacement of a horizontal zone. In the second model two apparently contradictory shear displacements result during major top-to-the-right shear in the horizontal zone. Given recognition of the well developed nature and continuity of Mc shear planes, and relatively minor left-lateral offset between megacryst fragments, the second model best fits the textures observed in the mylonite fabric. Acceptance of the second model indicates top-to-the-east displacement during mylonitic deformation of Okanogan dome rocks.

Further support of this relationship is given by documenting preferred rotation of megacrysts in sections parallel to M1 and lack of rotation in sections normal to M1. Table I summarizes clockwise versus counterclockwise rotation of megacrysts in these sections taken from traverse A. Interpretation of megacryst rotation is based on the following assumptions: 1) feldspar megacrysts are rigid bodies in a ductile deforming matrix; 2) the smaller portions of a megacryst rotate more than the larger portions of the same megacryst; and 3) deformation is not random in these rocks and the resulting deformation paths of several grains, or parts of grains, must be coherent or internally consistent with one another. Based on these assumptions I interpret grain rotations; Figure 6.8 pictures a fractured megacryst with arrows showing interpreted rotation direction. As seen from Table I, clockwise rotation dominates in sections parallel to M1 whereas no preferred rotation is seen in sections normal to M1. This relationship illustrates that the mylonitic lineation in these rocks could^{not} have formed as a result of rotation parallel to lineation as

proposed by Lister and Price (1978). Rotation on axes normal to M1 requires that shear, or tectonic transport, parallel M1. Clockwise rotation, viewed northward, of these rigid megacryst indicates right-lateral shear (Beck, 1980) (Fig. 11). Minor examples of counterclockwise rotation are observed in sections parallel to M1 (Table I). Given the heterogenous nature of the parent rock, on the scale of a thin section, opposite rotation is expected of a few grains; however, the dominant rotation should reflect overall sense of shear within the mylonite zone.

Megacryst imbrication and rotation document a similar sense of shear within the Okanogan mylonite, and both indicators are present and consistent throughout the zone studied. An even more pervasive and consistent shear indicator is interpreted from the Mc-Mm planes and their resulting asymmetry.

From the discussion above it is clear that Mm planes are short and discontinuous relative to Mc, although Mm planes deform Mc. Mc, in turn, deforms Mm. Therefore, these planes were active simultaneously for at least a portion of their movement histories; apparent shear on each respective surface is pictured in Figure 9. Mc shows apparent right-lateral displacement whereas Mm shows apparent left-lateral displacement. The interpretation of simultaneous movement is also supported by the parallel trend of M1 and M1' observed in the field. In summary, shear surfaces Mc and Mm moved at the same time, yet given apparently opposite senses of shear. Therefore the major plane of shear must be identified to determine an overall direction of

shear during mylonitic deformation of these rocks.

I propose Mc as the major plane of shear, proceeding from the following observations: 1) Mc is more continuous than Mm on both mesoscopic and microscopic scales; 2) Mc contains a more continuous lineation than Mm; 3) small measurable offset of megacrysts along Mm indicates minor movement occurred along Mm whereas no parts of megacrysts can be matched along Mc; the inference here is that displacement along Mc is greater than the field of view; and 4) offset of megacrysts along Mm is invariably contained between Mc planes, and can therefore not account for major shear of the mylonite. Accepting the proposal that the major plane of shear parallels Mc, the interpreted shear couple shows right-lateral displacement, viewed northward, to top-to-the-east displacement during formation of the Okanogan mylonite zone.

The Mc and Mm planes discussed above are similar to mylonitic textures described in the literature for other areas. Mc, representing major mylonitic foliation, corresponds to: "C" surfaces of Berthe et al (1979a, 1979b); mylonitic foliation, Sm, of White et al (1980); and foliation, S, of Platt and Visser (1980). In each of the above areas this plane of mylonitic foliation, Mc, C, Sm, and S, is a plane of major movement, parallel to the overall shear couple. Mm planes, sharp planar discontinuities cutting across mylonitic foliation at an acute angle, are similar to "S" surfaces of Berthe et al (1979a, 1979b) and crenulation zones of Platt and Visser (1980), and may be confused with shear bands, Ss, of White et al (1980). Figure 12 illustrates the relationship of these surfaces.

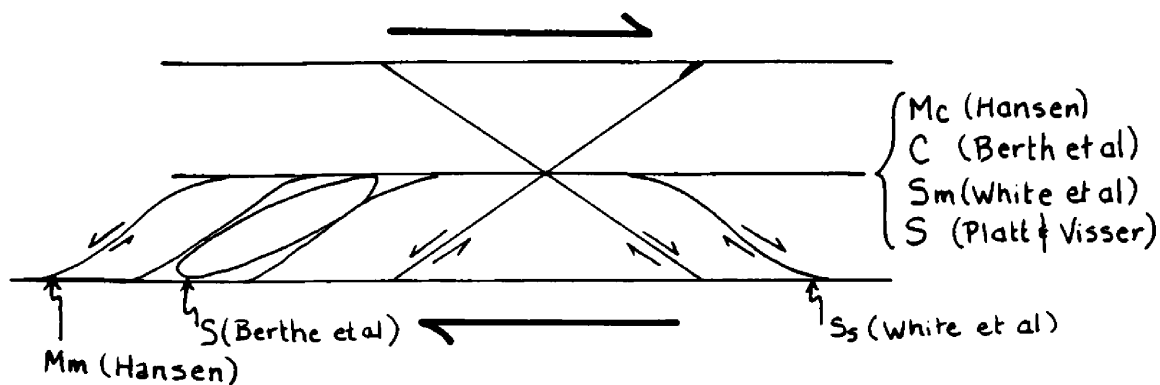


FIG. 12. "Crenulation zone" of Platt and Visser is similar to M_m (Hansen) and S_s (White et al) depending on the conditions of mylonitic deformation (see Platt and Visser, p. 406-408).

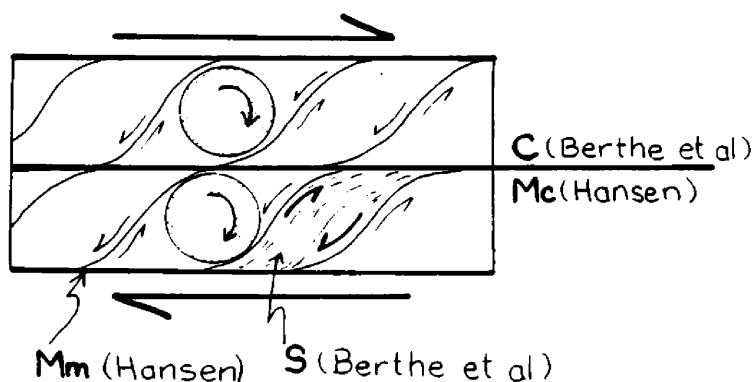


FIG. 13. Comparison of M_m (Hansen) and S (Berthe et al). If the crenulation zone is defined as the sharp discontinuous surface, M_m , left-lateral offset is observed; if the crenulation zone is defined as a broad zone, for example a mica lath, the zone shows right-lateral displacement, or clockwise rotation.

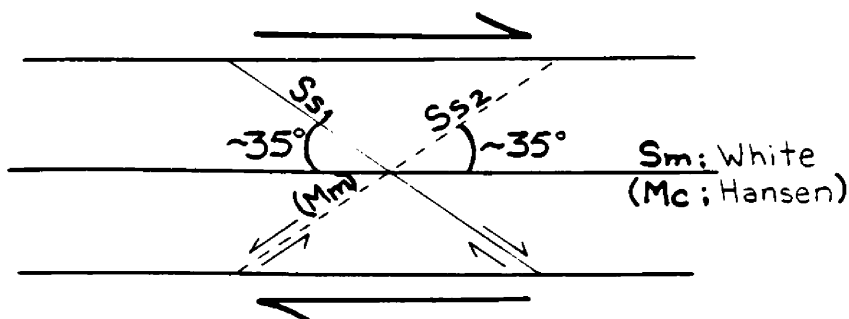


FIG. 14. Comparison of M_m (Hansen) and S_{s1} and S_{s2} (White).

Mc and Mm surfaces of this paper and C and S surfaces of Berthe et al (1979a, 1979b) are similar in their relationship to one another, and to the interpreted direction of shear. However, an important difference exists in the pairs of surfaces. According to Berthe et al, their S surfaces contain the maximum extension direction of the deformed minerals, and correspond to the XY plane of the finite strain ellipsoid during the initial stages of deformation. Whereas Berthe et al define S surfaces as zones of elongation, or minor right-lateral shear viewed northward, Mm surfaces of Okanogan mylonites are clearly planes of left-lateral shear, viewed in the same orientation. I believe this apparent difference reflects the scale of observation (Fig. 13). If the crenulation zone is defined as the sharp discontinuous surface, Mm, the apparent offset along that surface should be left-lateral relative to the other structures as in Figure 13. If the crenulation zone is defined as a broad zone, for example a thick mica lath (Berthe et al, 1979a, 1979b), the zone shows right-lateral shear or clockwise rotation as pictured in Figure 13. Offset on the sharp discontinuous surfaces is internally consistent with deformation within the zone between these sharp surfaces; the fabric interpretation presented in this paper is consistent with the fabric interpretation of Berthe et al (1979a, 1979b). Both surfaces, Mm and S, rotate toward mylonitic foliation, decreasing the acute angle between the crenulation zone and mylonitic foliation (Berthe et al, 1979a, 1979b; Platt and Visser, 1980).

Mm in Okanogan mylonites and Ss of White et al (1980) represent apparently opposite sets of shear bands which develop during progressive mylonitic deformation (Fig. 14) (see Platt and Visser, 1980; p. 406-408 for discussion; White, 1979a). Before accepting a kinematic interpretation of petrofabrics developed during mylonitic deformation, a worker must understand which fabrics are present in the rocks analyzed; it may be most valuable to check several types of textural evidence for consistent interpretation throughout a zone of mylonitization.

In summary, the Okanogan mylonite formed in a shear zone as defined by Ramsey and Graham (1970); deformation of the Okanogan dome was dominated by progressive simple shear and formed during eastward displacement of upper plate rocks with respect to lower plate rocks as shown by: 1) offset of pegmatites; 2) stretching of schistose inclusions; 3) imbrication of feldspars, the domino effect; 4) clockwise rotation of feldspar megacrysts, viewed northward, on axes normal to mylonitic lineation; and 5) the angular relationship of Mc and Mm surfaces, and their resulting asymmetry.

CHEMISTRY

Structural elements as well as metamorphic conditions define the environment of mylonitic deformation, and hence dome evolution. As discussed below coexisting feldspar mineralogy indicates that the Okanogan mylonite formed under middle-greenschist facies conditions.

In order to evaluate metamorphic conditions of mylonitization I studied chemical changes accompanying progressive mylonitization of a homogeneous granodiorite. I collected samples for whole-rock major-element analysis and oriented samples for detail mineral analysis along traverses through the Okanogan mylonite zone (Fig. 3). Samples for whole-rock chemical analysis were collected at alternate stations; oriented samples were collected at every station. Whole-rock major-element analyses should record macroscopic chemical changes through the mylonite zone and microprobe analyses should record detailed chemical trends within specific minerals; biotite and feldspars were analyzed.

Whole-rock major-element analyses were determined by X-ray fluorescence spectrometry. Mineral analyses were performed on a Cameca computer automated microprobe. Analyses were performed on wavelength spectrometers with absorbed current of 5.5 nA. Oxide weight percent values and normative minerals are calculated from normalized atomic concentrations. Normalized element and oxide values for biotite are anhydrous.

Whole-rock major-element analyses and specific gravity determinations (Table II) indicate that no major chemical changes took place with progressive mylonitization of megacrystic granodiorite; thus, on a macroscopic scale mylonitization involved constant volume and isochemical deformation.

FELDSPAR MINERALOGY

Although progressive mylonitization of megacrystic granodiorite is isochemical on a macroscopic scale, feldspars on a microscopic scale exhibit important chemical trends. Feldspar grains show signs of both brittle and ductile deformation; fracturing and breakage indicate dominantly brittle processes (Lister and Price, 1978; Watts and Williams, 1979), and segregation bands with associated kinking and microfracturing indicate dominantly ductile processes (Hanmer, 1981, 1982). Very fine new grains develop along the borders of feldspar megacrysts and original grains become progressively rounded and smaller; this fine-grained recrystallization may involve both dislocation movement and strain-enhanced diffusion (Allison et al, 1979; Barnett and Kerrich, 1980; Etheridge and Hobbs, 1974; Kerrich et al, 1980; White, 1976). The goal of this portion of my study is to record chemical trends across such recrystallized feldspar grains and to use the percent albite component of coexisting recrystallized feldspars to estimate a temperature of their recrystallization during mylonitization (after Stormer, 1975; Powell and Powell, 1977).

Tables III, IV, and V record major-element microprobe analyses and normative Ab, An, and Or calculations from plagioclase (III) and orthoclase (IV) megacryst cores to rims, and very fine-grained recrystallization surrounding host grains, and coexisting recrystallized feldspar pairs (V). Ab, An, and Or components, of plagioclase and orthoclase megacryst cores and fine-grained recrystallized grains, are plotted on a ternary diagram in Figure 15. From core to rim to

recrystallized matrix grains, plagioclase gains Ab component and loses An and Or component. Kerrich et al (1980) and Hanmer (1982) report similar trends in mylonitized plagioclase. Orthoclase grains gain Or and lose Ab component in traverses from core to rim to recrystallized matrix. This change is similar to that for orthoclase reported by Kerrich et al, but in contrast to that of Hanmer who reports a gain in Ab component in mylonitized orthoclase.

Given that diffusion of alkalis is an important process in feldspar recrystallization during mylonitic deformation (Allison et al, 1979; Hanmer, 1981, 1982; Kerrich et al, 1980) the chemical composition of coexisting recrystallized feldspar pairs ought to "lock in" information on the environment during mylonitization. The proportion of Ab component in coexisting feldspar pairs should give an estimate of temperature of mylonitization (Stormer, 1975; Stormer and Whitney, 1975; Whitney and Stormer, 1975). The assumption that diffusion plays an important role in feldspar recrystallization during mylonitization is reasonable considering the intimate interaction of dislocation mobility and diffusion during mylonitization (Allison et al, 1979; Barnett and Kerrich, 1980; Beach, 1980; Brodie, 1980; Etheridge and Hobbs, 1974; Herrich et al, 1980; White, 1976). Increase in shearing stress markedly increases diffusion and reaction rates for mineralogical changes (Dachille and Roy, 1964) and rates of deformation by dislocation movements (Tullis et al, 1973). In essence, dislocation deformation and diffusion metamorphism speed a system toward chemical equilibrium with its environment.

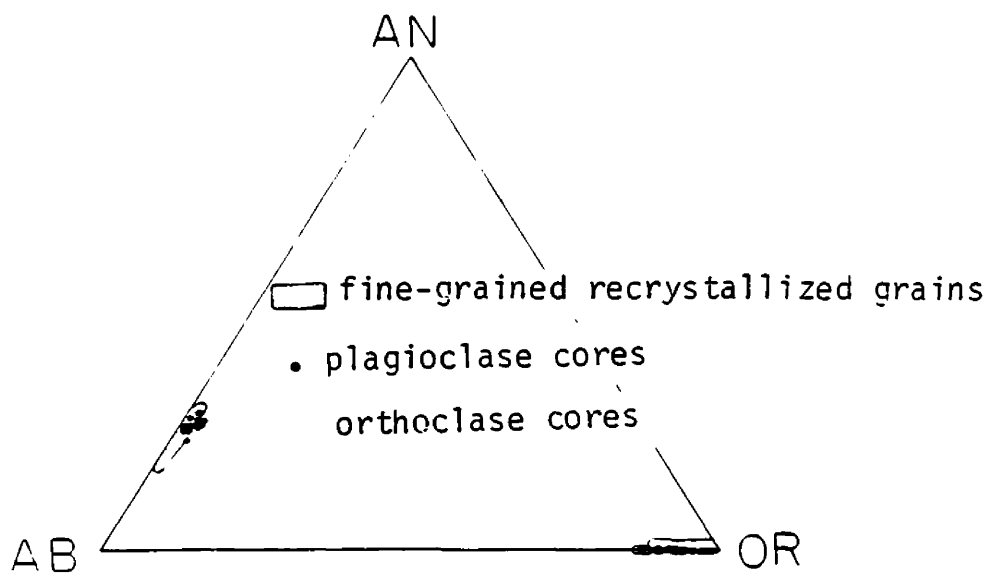


FIG. 15. Ternary diagram of Ab, An, and Or in plagioclase and orthoclase megacryst cores and fine-grained recrystallized matrix.

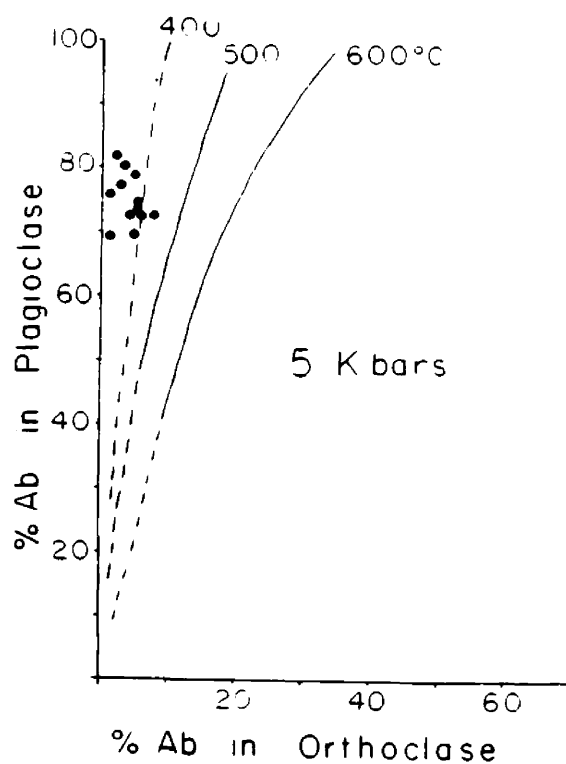


FIG. 16. Percent Ab in fine-grained recrystallized coexisting plagioclase and orthoclase (graph after Stormer, 1975).

Figure 16 is a plot of percent Ab in fine-grained recrystallized coexisting plagioclase and orthoclase taken from rocks throughout the mylonite zone along traverse A. Coexisting feldspar pairs form a tight cluster of points just below 400°C on the 5 kbar plot generated by Stormer (1975). I chose to plot the data on the 5 kbar plot based on Sibson's (1977) classification of fault rocks and mechanisms. Although the 400°C curve of Stormer (1975) is dashed and therefore of lesser confidence, the coexisting feldspar pairs plot well below this curve. This temperature of less than 400°C is in agreement with Kerrich et al (1980) who report similar chemical trends, and compositions, in mylonitized feldspars. They determined a mylonitization temperature of approximately 250°C ± 30°C as determined by fluid inclusion filling temperatures in syntectonic microveins, from 618 0 in quartz-ilmenite of +150/100, and from mineral stability criteria.

In summary, feldspar grains of granodiorite in the Okanogan mylonite show transitional behavior between ductile and brittle processes and exhibit consistent chemical trends with mylonitic deformation. Plagioclase gains Ab, and loses An and O4 during mylonitic recrystallization whereas orthoclase gains Or and loses Ab. A plot of percent Ab component in coexisting recrystallized feldspar pairs indicates a temperature of less than 400°C during mylonitization. This temperature corresponds to middle-greenschist facies conditions.

BIOTITE CHEMISTRY

Biotite from Mc and Mm surfaces throughout the mylonite zone along

traverse A were analyzed for major elements to determine whether chemical variations exist between Mc and Mm biotite. The presence of two distinctly different biotite compositions may indicate strain-induced chemical potential gradients within and across shear zones (Kerrick et al, 1980). Anhydrous, normalized atomic concentrations, oxide weight percentages, and Fe:Mg:Ti ratios are given in Table VI. Fe:Mg:Ti ratios of Mc and Mm biotite are plotted in Figure 17. Slight variations in biotite chemistry exist. However, no consistent trends in chemical change are present in comparison of: 1) biotite core to rim variations; 2) Mc versus Mm biotites; 3) increased mylonitic deformation of Mc biotite; or 4) increased mylonitic deformation of Mm biotite.

No major chemical differences exist in the cores of apparently undeformed biotite laths and finely recrystallized biotite of Mc and Mm. Therefore, either all biotite recrystallized to a similar composition, or biotite did not recrystallize during mylonitization. The fact that there is no detectable chemical difference between Mc and Mm biotite supports the hypothesis presented above that Mc and Mm were active simultaneously.

I conclude from the data presented above that the mylonite within the southwest sector of Okanogan dome formed under middle-greenschist facies conditions during eastward displacement of upper plate rocks relative to lower plate rocks. The mylonitic fabric is superimposed on an earlier regional high-grade metamorphism and associated deformation, and is cut by a later low-grade brittle deformation and

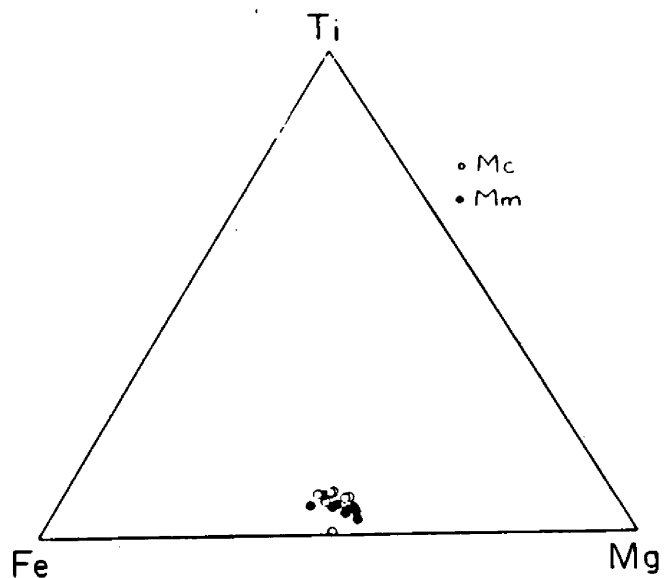


FIG. 17. Fe:Mg:Ti ratios of Mc and Mm biotite.

TABLE I



	Sample		
II to M ₁	11A	43	13
	10A	20	5
	9A	19	3
	8A	35	5
	7A	5	1
	6A	18	5
	5A	13	2
I to M ₁	11A'	6	5
	10A	2	1
	9A	4	4
	8A	2	0
	7A	0	3
	6A	1	1
	5A	1	2

TABLE II: Whole rock major element analyses

Analysis	inc. myl. def. →					inc. myl. def. →				- inc. myl. def. →			
	2A	4A	6A	8A	10A	2B	4B	6B	7B	2C	4C	6C	8C
SiO ₂	69.99	68.57	70.68	70.31	72.10	70.35	71.03	70.24	70.05	69.60	70.65	70.17	71.37
Al ₂ O ₃	17.54	18.35	17.42	17.27	16.62	17.55	16.83	17.14	17.26	17.75	17.17	17.38	16.82
TiO ₂	0.36	0.37	0.32	0.34	0.28	0.34	0.33	0.33	0.35	0.36	0.35	0.33	0.31
FeO	1.93	1.93	1.69	1.95	1.24	1.89	1.83	1.80	2.01	2.01	1.96	2.04	1.67
MnO	0.05	0.05	0.04	0.05	0.03	0.04	0.05	0.05	0.05	0.04	0.05	0.05	0.05
CaO	3.47	3.73	3.18	3.45	2.91	3.29	3.34	3.35	3.30	3.40	3.32	3.28	3.25
MgO	0.29	0.44	1.69	0.25	0.25	0.27	0.32	0.31	0.37	0.52	0.36	0.33	0.32
K ₂ O	1.79	1.86	1.82	1.76	2.59	2.18	1.99	2.33	2.42	2.01	1.93	2.06	2.02
Na ₂ O	4.46	4.52	3.09	4.47	3.88	3.96	4.11	4.31	4.03	4.20	4.04	4.22	4.09
P ₂ O ₅	0.13	0.17	0.08	0.16	0.11	0.13	0.16	0.14	0.16	0.12	0.17	0.15	0.10

TABLE III: Plagioclase

Analysis	increasing mylonitic deformation →											
	core 66	rim 67	rxl 68	rxl 76	core 77	rim 78	rxl 81	rxl 85	core 92	rim 91	rim 89	rxl 87
Si	20.925	20.903	21.255	22.109	20.640	20.842	21.052	20.756	20.791	20.852	21.421	21.782
Al	9.988	10.023	9.512	9.009	10.168	10.093	9.787	10.098	10.221	10.230	9.457	9.236
Ca	1.712	1.699	1.713	1.431	1.920	1.900	1.681	1.886	1.913	1.99	1.361	1.445
Na	5.743	5.789	5.970	5.449	5.733	5.575	5.935	5.726	5.352	5.137	6.192	5.766
K	0.143	0.102	0.049	0.076	0.148	0.053	0.077	0.084	0.147	0.110	0.056	0.016
O	61.488	61.484	61.501	61.925	61.392	61.537	61.470	61.450	61.576	61.672	61.513	61.754
SiO ₂	61.41	61.37	62.44	65.11	60.47	61.13	61.83	60.86	60.93	61.09	63.09	64.15
Al ₂ O ₃	24.87	24.97	23.71	22.51	25.28	25.12	24.39	25.12	25.41	25.43	23.63	23.08
CaO	4.69	4.66	4.70	3.93	5.25	5.20	4.61	5.17	5.23	5.47	3.74	3.97
Na ₂ O	8.69	8.77	9.05	8.28	8.66	8.43	8.99	8.66	8.09	7.76	9.41	8.76
K ₂ O	0.33	0.23	0.11	0.18	0.34	0.12	0.18	0.19	0.34	0.25	0.13	0.04
Ab	74.21	74.91	75.80	77.31	70.77	72.91	75.52	72.45	71.00	69.65	80.41	78.80
An	23.80	23.70	23.55	21.52	27.14	26.37	23.40	26.40	26.91	28.78	18.81	20.94
Or	1.99	1.39	0.66	1.17	2.09	0.73	1.08	1.15	2.09	1.57	0.78	0.26

TABLE IV: Orthoclase

Analysis	increasing mylonitic deformation →												
	core 74	rim 72	rim 70	rxl 69	rxl 75	core 36	rim 37	rim 40	rxl 42	rxl 44	core 20	rim 24	rxl 22
Si	22.704	22.767	22.669	22.611	22.852	22.706	22.728	22.818	22.692	22.726	22.751	22.828	22.864
Al	8.273	8.335	8.372	7.957	8.180	8.150	8.161	7.992	8.138	8.104	8.154	8.120	7.997
Ca	0.00	0.00	0.00	0.00	0.00	0.00	0.00	0.00	0.00	0.00	0.00	0.00	0.00
Na	0.922	0.892	0.363	1.005	0.228	1.097	0.667	0.698	0.409	0.539	1.045	0.787	0.422
K	6.548	6.349	7.012	7.179	7.101	6.574	6.942	7.013	7.311	7.169	6.530	6.690	7.189
O	61.553	61.657	61.584	61.248	61.639	61.473	61.502	61.479	61.450	61.462	61.520	61.575	61.528
SiO ₂	64.26	64.54	63.93	63.68	64.41	64.25	64.13	64.35	63.85	64.02	64.40	64.54	64.40
Al ₂ O ₃	19.87	20.05	20.03	19.01	19.56	19.57	19.54	19.12	19.43	19.37	19.58	19.48	19.11
CaO	0.00	0.00	0.00	0.00	0.00	0.00	0.00	0.00	0.00	0.00	0.00	0.00	0.00
Na ₂ O	1.35	1.30	0.53	1.46	0.33	1.60	0.97	1.02	0.59	0.78	1.53	1.15	0.61
K ₂ O	14.53	14.11	15.50	15.85	15.69	14.58	15.36	15.51	16.13	15.83	14.49	14.83	15.87
Ab	11.74	11.65	4.66	1.17	2.92	11.92	7.68	6.69	2.18	4.29	13.14	9.99	5.21
An	0.00	0.00	0.00	0.00	0.00	0.00	0.00	0.00	0.00	0.00	0.00	0.00	0.00
Or	88.26	88.35	95.34	98.83	97.08	88.08	92.32	93.31	97.82	95.71	86.86	90.91	94.79

TABLE VI: Biotite

Analysis	core → rim			core → rim			Mn biotite: inc. myl. def. →						Mc biotite: inc. myl. def. →					
	5	9	8	25	26	27	47	14	21	46	36	24	52	4	19	39	35	23
Si	14.797	14.773	14.899	14.525	14.643	14.899	14.690	14.927	14.506	14.959	14.689	14.445	14.822	14.823	14.807	14.863	14.584	14.626
Al	7.363	7.465	7.605	7.229	7.896	8.305	6.948	8.334	7.525	7.921	7.574	7.246	6.910	8.051	7.445	7.656	7.287	7.484
Ti	0.965	0.931	0.968	0.906	0.793	0.543	1.096	0.724	0.982	0.626	0.857	1.010	0.959	0.977	0.943	1.150	1.176	0.926
Fe	6.516	6.675	5.845	6.626	6.003	5.497	7.264	6.358	6.564	6.019	7.451	6.703	7.135	5.968	6.466	6.342	7.070	6.529
Mg	6.690	6.535	6.925	7.176	6.922	7.233	6.374	6.137	6.689	6.777	6.059	6.911	6.521	6.437	6.830	6.064	6.136	6.928
Mn	0.110	0.091	0.088	0.262	0.232	0.165	0.219	0.087	0.214	0.193	0.174	0.268	0.203	0.100	0.167	0.183	0.192	0.260
Ca	0.000	0.000	0.000	0.000	0.000	0.000	0.000	0.000	0.000	0.000	0.000	0.000	0.000	0.000	0.000	0.000	0.000	0.000
Na	0.120	0.010	0.067	0.029	0.113	0.034	0.069	0.019	0.034	0.113	0.000	0.064	0.212	0.099	0.048	0.114	0.136	0.000
K	5.021	5.072	5.049	4.976	4.980	4.715	4.971	4.678	5.158	4.864	4.687	6.911	4.897	4.876	4.760	4.982	5.000	4.801
O	58.430	58.448	58.556	58.271	58.419	58.610	58.370	58.735	58.327	58.529	58.499	58.247	58.340	58.669	58.534	58.646	58.418	58.447
SiO ₂	38.22	38.08	38.83	37.41	38.08	39.21	37.46	38.81	37.34	39.00	37.57	37.10	37.95	38.60	38.32	38.39	37.28	37.76
Al ₂ O ₃	16.14	16.32	16.82	15.80	17.42	18.54	15.04	18.39	16.44	17.52	16.43	15.79	15.01	17.79	16.35	16.78	15.81	16.39
TiO ₂	3.27	3.19	3.35	3.10	2.74	1.90	3.72	2.50	3.36	2.17	2.91	3.45	3.27	3.38	3.25	3.95	4.00	3.18
FeO	20.12	20.57	18.21	20.41	18.67	17.30	22.17	19.77	20.20	18.76	22.78	20.58	21.88	18.58	20.01	19.59	21.61	20.16
MgO	11.59	11.30	12.11	12.40	12.08	12.77	10.91	10.71	11.55	11.85	10.39	11.91	11.20	11.25	11.86	10.51	10.52	12.00
MnO	0.34	0.28	0.27	0.80	0.71	0.51	0.66	0.27	0.65	0.59	0.53	0.81	0.61	0.31	0.51	0.56	0.58	0.79
Na ₂ O	0.16	0.01	0.09	0.04	0.15	0.05	0.09	0.03	0.05	0.15	0.00	0.08	0.28	0.13	0.06	0.15	0.18	0.00
K ₂ O	10.17	10.25	10.32	10.05	10.15	9.73	9.94	9.53	10.41	9.94	9.39	10.28	9.83	9.95	9.66	10.09	10.02	9.72
Fe	46.02	47.20	42.55	45.05	43.76	41.42	49.30	48.10	46.11	44.84	51.86	45.84	48.82	44.60	45.41	46.78	49.16	45.40
Mg	47.25	46.22	50.41	48.79	50.46	54.50	43.26	46.43	46.99	50.49	42.18	47.26	44.62	48.10	47.97	44.74	42.66	48.17
Ti	6.72	6.58	7.04	6.16	5.79	4.09	7.44	5.48	6.90	4.67	5.96	6.90	6.56	7.30	6.63	8.48	8.18	6.44

TABLE V: Coexisting feldspars

Analysis	increasing mylonitic deformation →															
	31	34	53	54	75	76	64	65	84	85	42	41	88	89	22	23
Si	22.890	20.925	23.229	20.860	22.852	22.109	22.646	20.624	22.749	20.756	22.692	23.095	22.902	21.421	22.864	21.053
Al	8.030	9.951	7.412	9.998	8.180	9.009	8.199	10.219	8.320	10.098	8.138	8.098	8.084	9.457	7.997	9.851
Ca	0.000	1.914	0.000	1.899	0.000	1.431	0.000	2.117	0.000	1.886	0.000	1.069	0.000	1.361	0.000	1.769
Na	0.613	5.605	0.760	5.673	0.228	5.449	0.629	5.481	0.440	5.726	0.409	5.486	0.263	6.192	0.422	5.683
K	6.891	0.074	7.095	0.079	7.101	0.076	7.081	0.083	6.863	0.084	7.311	0.069	7.127	0.056	7.189	0.101
O	61.576	61.531	61.504	61.491	61.639	61.925	61.445	61.476	61.629	61.450	61.450	62.183	61.624	61.513	61.528	61.543
SiO ₂	64.62	61.36	65.49	61.17	64.41	65.11	63.83	60.37	64.23	60.86	63.85	68.23	64.54	63.09	64.40	61.79
Al ₂ O ₃	19.23	24.76	17.73	24.87	19.56	22.51	19.61	25.38	19.93	25.12	19.43	20.30	19.33	23.63	19.11	24.53
CaO	0.00	5.24	0.00	5.20	0.00	3.93	0.00	5.78	0.00	5.17	0.00	2.95	0.00	3.74	0.00	4.85
Na ₂ O	0.89	8.48	1.11	8.58	0.33	8.28	0.91	8.27	0.64	8.66	0.59	8.36	0.38	9.41	0.61	8.60
K ₂ O	15.25	0.17	15.68	0.18	15.69	0.18	15.65	0.19	15.19	0.19	16.13	0.16	15.75	0.13	15.87	0.23
Ab	7.71	72.66	4.04	72.65	2.92	77.31	4.87	69.57	5.70	72.45	2.18	81.94	3.34	80.41	5.21	74.11
An	0.00	26.33	0.00	26.27	0.00	21.52	0.00	29.29	0.00	26.40	0.00	16.97	0.00	18.81	0.00	24.50
Or	92.29	1.01	95.96	1.08	97.08	1.17	95.13	1.14	94.31	1.15	97.82	1.10	96.66	0.77	94.79	1.39

associated deformation, and is cut by a later low-grade brittle deformation and associated chloritization (Snook, 1965; Goodge, 1983; Goodge and Hansen, in press; Hansen, 1981).

CONCLUSIONS

Okanogan dome displays many characteristics suggestive of diapiric emplacement: 1) smooth sharp outer boundaries; 2) strong foliation developed in dome rocks generally parallels the dome boundaries; and 3) maximum deformation within the dome is present at the margins and disappears toward the dome interior (see Pitcher and Berger, 1972). Despite these similarities with documented examples of diapiric rise, the Okanogan dome mylonite displays an important difference. Although the mylonitic foliation parallels the dome boundaries, the accompanying lineation is unidirectional throughout the dome, regardless of the dip of the foliation, and does not form steeply plunging radial lineations as in documented examples of diapiric emplacement.

The relationship of mylonitic foliation parallel to the dome margin, together with unidirectional lineation are best explained with a two-phase model of dome evolution. A sub-horizontal mylonite zone formed as an intracontinental shear zone during eastward displacement of upper-plate rocks, in a direction parallel to mylonitic lineation. Granitoid rocks deformed in the shear zone included biotite-megacryst granodiorite of this study which intruded amphibolite-grade crystalline rocks. Later doming gently warped the 1 to 1.5 km thick mylonite zone causing mylonitic foliation to parallel the late dome borders, yet preserved

the earlier-formed unidirectional mylonitic lineation. This doming was accompanied by brecciation and chloritization which overprints the mylonitic fabric, and probably occurred during the documented Tertiary thermal event (Armstrong et al, 1977; Matthews, 1981; Medford, 1975; Miller and Engels, 1975; Ross, 1974, 1975) which reset K-Ar dates to 50 to 60 Ma within the dome boundaries (Fox et al, 1977).

TECTONIC FRAMEWORK

The relative timing of geologic events and kinematic interpretation of mylonitic deformation of Okanogan dome rocks is strikingly similar to the geologic and kinematic history proposed for the Monashee complex (Brown and Murphy, 1982; Read and Brown, 1981). These workers propose that the unidirectional east-west-trending mylonitic fabric in the Columbia River fault zone formed during eastward displacement of the hanging wall relative to the foot wall, following the peak of regional high-grade metamorphism; younger motion on the Columbia River fault induced gentle macroscopic folding and brecciation of the mylonitic layering. Similar-trending unidirectional mylonitic lineation and interpreted top-to-the-east displacement are also present in the Kettle (?), Spokane (Rhodes, 1983), and Bitterroot (Hyndman, 1980) domes (Fig. 1). In these domes brittle deformation and associated chloritization are also documented as post-dating mylonitization.

Similarities in these tectonic features and their kinematic interpretation suggest a related tectonic origin. Templeman-Kluit (1979), and Mattauer et al (1983) and Brown and Read (1983) propose

similar tectonic models for the northern-most Cordillera in the Yukon and the Shuswap complex respectively. These models address the pervasive unidirectional transverse lineation, recumbent folding, and eastward thrusting. These workers relate the mylonite zones to large-scale intracontinental alpine-type eastwardly directed shear zones resulting from the Jurassic collision of the Stikine block with the North American craton. A Tertiary thermal event caused arching, uplift and normal faulting. This causes brittle reactivation of parts of old ductile shear zones, exposing core rocks, and resetting K-Ar dates to Eocene ages. The conclusions of this study are consistent with the constraints of these similar tectonic models, although no absolute dates for Okanogan events are determined.

I propose that the tectonic model of Mattauer et al (1983) be extended westward, and the tectonic models of Templeman-Kluit (1979) and Brown and Read (1983) be extended southward to include Okanogan dome. The amalgamated Stikine and Quesnellia blocks (see Monger et al, 1982) collided with the North American plate during west-dipping subduction during Late Triassic-Early Jurassic time (Templeman-Kluit, 1979). Templeman-Kluit (1979) recognizes the Teslin Suture, a northwest-trending 15 km-thick zone of steeply dipping variably deformed cataclastic and mylonitic rock, as the arc-continent suture zone in southwestern Yukon Territory. Farther south, in central British Columbia, Struik (1981) identifies a Late Triassic-early Jurassic mylonite zone, separating allochthonous Quesnellia from the Shuswap terrain of the North American plate to the east, marking the arc-continent suture.

An arc-continent suture of Late Triassic-Early Jurassic has not been identified in southern British Columbia and northern United States although Triassic oceanic metasedimentary rocks include serpentinite bodies elongate parallel to metamorphic foliation crop out west of Okanogan dome (Rinehart and Fox, 1976) and may represent dissected remains of an arc-continent suture. Lens-shaped metamorphic (?) dunite bodies are also enclosed in the high-grade paragneiss assemblage (pgn) southwest of Okanogan dome (Fig. 3) (see Goodge and Hansen, in press). These ultramafic bodies were probably emplaced as tectonic slivers of serpentinite prior to high-grade regional metamorphism and may mark an ancient melange or suture to the west of the present Okanogan dome.

The Late Triassic-Early Jurassic arc-continent suture should lie west of, and structurally above the Okanogan mylonite. The ancient suture may be difficult to identify as the zone was metamorphosed and folded with arc-continent collision during Early to Middle Jurassic time, and later thrust eastward over the North American plate margin (Templeman-Kluit, 1979; Struik, 1981; Brown and Read, 1983; Mattauer et al, 1983).

During Middle- to Late-Jurassic time the North American plate began to underplate the accreted composite arc terrain to the west. This underplating caused eastward thrusting of the suture zone over the North American plate (Templeman-Kluit, 1979; Struik, 1981; Brown and Read, 1983) and associated development of large-scale easterly directed intracontinental shear zones within the North American plate (Templeman-Kluit, 1979; Mattauer et al, 1983). Examples include the

Monashee decollement (Brown and Read, 1983) and the Okanogan, Kettle, Spokane, and Bitterroot dome mylonite zones.

The nature of the Late-Triassic-Early Jurassic ductile deformation of rocks in the 15 km-thick Teslin suture is markedly different from the gently-dipping, relatively thin mylonite zones of the Monashee decollement, and Okanogan, Kettle, Spokane, and Bitterroot domes. This difference lies in the fact that the Teslin suture marks a suture zone between arc and continent, whereas the relatively thin mylonite zones mark deep-seated shear zones contained within the North American plate. In comparison with the Himalayan model the Teslin Suture corresponds to the Indus Suture between the collided continents, and the Monashee decollement and similar mylonite zones correspond to the Main Central and Main Boundary Thrusts (Ganser, 1964).

Eastward displacement along deep-seated intracontinental shear zones continued through Cretaceous time though timing of specific shear zones varies (Brown and Read, 1983; Mattauer et al, 1983). Ductile movement on the Monashee decollement ended during Late Jurassic time whereas eastward displacement probably continued on a sole fault beneath the Monashee complex (Brown and Read, 1983). The Okanogan mylonite zone may be continuous with the Monashee decollement, or it may mark the trace of a deeper sole fault with movement continuing through Cretaceous time. No absolute ages are available for the Okanogan mylonite. Final movement on intracontinental shear zones carried crystalline slabs eastward relative to the North American craton. This resulted in shortening to the east and formation of the

Rocky Mountain fold and thrust belt in the south and the Mackenzie Mountains in the north (Templeman-Kluit, 1979; Brown and Read, 1983; Mattauer et al, 1983).

Major compressional tectonics ended by Late Cretaceous-Early Tertiary time (Hyndman, 1980), followed by Eocene extensional tectonics (Cheney, 1980; Ewing, 1981; Read and Brown, 1981; Rhodes and Cheney, 1981). The well-documented Eocene thermal event caused doming of the intracontinental shear zones and their associated infrastructure, development of normal faults, and resetting of K-Ar dates (Read and Brown, 1981; Miller and Engels, 1975; Fox et al, 1977; Brown and Murphy, 1982; Cheney, 1980).

Southwest of the Okanogan dome southwest-dipping normal faults cut Tertiary (?) dikes (Goodge and Hansen, in press) and Eocene volcanic rocks west of the dome (Rinehart and Fox, 1976). Within the Okanogan dome prominent north-south-trending joints cut the mylonitic rocks and are locally intruded by Tertiary (?) microdiorite dikes (Goodge and Hansen, in press).

The documented Eocene thermal event reflects anomalously high heat flow which may result from extensive Eocene volcanism and plutonism. LaFort (1981) outlines a model for magma generation due to post-collision basement thrusting in the Himalayas. LaFort's model for leucocratic magma generation provides a possible explanation for the Cordilleran Eocene thermal event. Tectonic burial by northward underthrusting of the relatively cold and wet Tibetan sedimentary series by the relatively hot Tibetan slab caused prograde metamorphism

of the sedimentary rocks and release of fluids which induced partial melting of the overlying Tibetan slab to produce leucocratic magma. Final movement on the lower-most intracontinental fault of the Cordillera could have placed a relatively hot crustal slab over relatively cold and wet sedimentary rocks to the east. This could cause prograde metamorphism of the underplated North American sediments, resulting release of fluids, and anatexis of the overlying crystalline slab. Tertiary siliceous magmas of north-central Washington may have been generated in this manner and may be responsible for the recorded Eocene high-heat flow and reset K-Ar dates. Magma emplacement could cause the documented crustal extension resulting in rapid uplift and development of normal faults, exposing intracontinental mylonite zones and their associated suprastructure now exposed.

Therefore, the Cordilleran Eocene thermal event of north-central Washington may result, at least in part, from Tertiary production of leucogranite by postcollisional easterly directed basement thrusting over cool, wet sedimentary rocks of the North American plate. Metamorphic release of fluids from the underlying sediments, and rise of these fluids into the overlying plate would cause partial melting of the overlying crustal slab.

In summary, the geologic conclusions of this study are consistent with the constraints of tectonic models of Cordilleran evolution presented by Templemen-Kluit (1979), Brown and Read (1983), and Mattauer et al (1983). The tectonic models proposed by these workers

are similar to Himalayan-type collision orogen. In addition, I propose that the Himalayan-type model of magma generation (after LaFort, 1981) may be a viable model for postcollision magma generation responsible for the Cordilleran Eocene thermal event of north-central Washington.

REFERENCES CITED

- Allison, I., Barnett, R. L., and Kerrich, R., 1979, Superplastic flow and changes in crystal chemistry of feldspars: *Tectonophysics*, 53, pp. T41-T46.
- Allison, I. and Latour, T. B., 1977, Brittle deformation of hornblende in a mylonite: *Canadian Journal of Earth Science*, 14, pp. 1953-1958.
- Armstrong, R. L., Taubeneck, W. H. and Hales, P. Q., 1977, Rb/Sr and K/Ar geochronometry of Mesozoic granitic rocks and their isotopic composition, Oregon, Washington and Idaho: *Geological Society of America Bulletin*, 88, pp. 379-411.
- Barnett, R. L. and Kerrich, R., 1980, Stress corrosion cracking of biotite and feldspar: *Nature*, 283, pp. 185-187.
- Beach, A., 1980, Retrogressive metamorphic processes in shear zones with special reference to the Lewisian complex: *Journal of Structural Geology*, 2, pp. 257-263.
- Beck, M. E., Jr., 1980, Paleomagnetic record of plate-margin tectonic processes along the western edge of North America: *Journal of Geophysical Research*, 85, pp. 7115-7131.
- Bell, T. H. and Etheridge, M. A., 1973, Microstructure of mylonites and their descriptive terminology: *Lithos*, 6, pp. 337-348.
- Berthe, D., Choukroune, P. and Gapais, D., 1979, Orientations preferentielles du quartz et orthogneissification progresseve en regime cisailant: l'exemple due cisaillement sud amoricain: *Bull. Mineral.*, 102, pp. 265-272.
- Berthe, D., Choukroune, P., and Jegouzo, P., 1979, Orthogneiss, mylonite and non coaxial deformation of granites: the example of the south Armorican shear zone: *Journal of Structural Geology*, 1, pp. 31-42.
- Brodie, K. H., 1980, Variations in mineral chemistry across a shear zone in phlogophite peridotite: *Journal of Structural Geology*, 2, pp. 265-272.
- Brown, R. L. and Read, P. B., 1983, Shuswap terrane of British Columbia: A Mesozoic "core complex": *Geology*, 11, pp. 164-168.

- Brown, R. L. and Murphy, D. C., 1982, Kinematic interpretation of mylonitic rocks in part of the Columbia River fault zone, Shuswap terrane, British Columbia: Canadian Journal of Earth Science, 19, pp. 456-465.
- Cheney, E., 1980, The Kettle dome and related structures of north-eastern Washington, in: Crittenden, M. D. et al (eds), Cordilleran Metamorphic Core Complexes: Geological Society of American Memoir 153, pp. 465-484.
- Crittenden, M. D., Jr., Coney, P. J. and Davis, G. H., 1980, Cordilleran Metamorphic Core Complexes: Geological Society of America Memoir 153, 490 pp.
- Dachille, F. and Roy, R., 1964, Effectiveness of shearing in accelerating solid phase reactions at low temperature and high pressure: Journal of Geology, 72, pp. 243-247.
- Davis, G. H. and Coney, P. J., 1979, Geologic development of the Cordilleran metamorphic core complexes: Geology, 7, pp. 120-124.
- Debat, P., Soula, J. C., Kubin, L. and Vidal, J. L., 1978, Optical studies of natural deformation microstructures in feldspars (gneiss and pegmatite from Occitania, southern France): Lithos, 11, pp. 133-145.
- Etheridge, M. A., and Hobbs, H. B., 1974, Chemical and deformational controls on recrystallization of mica: Contributions to Mineralogy and Petrology, 43, pp. 111-124.
- Ewing, T. E., 1981, Paleogene tectonic evolution of the Pacific Northwest: Journal of Geology, 88, pp. 619-638.
- Fox, K. F., Jr., Rinehart, C. D. and Engels, J. C., 1977, Plutonism and Orogeny in North-central Washington--Timing and Regional Context: U. S. Geological Survey Professional Paper 989, 27 pp.
- Fox, K. F., Jr., Rinehart, C. D., Engels, J. C., and Stern, T. W., 1976, Age of emplacement of the Okanogan gneiss dome north-central Washington: Geological Society of America Bulletin 87, pp. 1217-1224.
- Fox, K. F., Jr., and Rinehart, C. D., 1971, Okanogan gneiss dome (abs.), in: Metamorphism in the Canadian Cordillera: Vancouver, British Columbia, Canada Geological Association, Cordilleran Section, Program and Abstracts, p. 10.
- Gansser, A., 1964, Geology of the Himalayas, Interscience, New York; 289 pp.

- Goodge, J. W., 1983, Reorientation of folds by progressive mylonitization, Okanogan dome, north-central Washington: Geological Society of America Abstracts with Programs, 15, 5, p. 323.
- Goodge, J. W., and Hansen, V. L., in press, Petrology and structure of rocks in the southwest portion of Okanogan dome, north-central Washington: Northwest Geology.
- Hanmer, S. K., 1983, Microstructure and geochemistry of plagioclase and microcline in naturally deformed granite: Journal of Structural Geology, 4, pp. 197-213.
- _____, 1981, Segregation bands in plagioclase: non-dilational enechelon quartz veins formed by strain enhanced diffusion: Tectonophysics, 79, pp. T53-T61.
- Hansen, V. L., 1983, Kinematic interpretation of mylonitic rocks in the Okanogan dome, north-central Washington: Geological Society of America Abstracts with Programs, 15, 5, p. 323.
- Hibbard, M. J., 1971, Evolution of a plutonic complex, Okanogan Range, Washington: Geological Society of America Bulletin 82, pp. 3013-3047.
- Hobbs, B. E., 1981, The influence of metamorphic environment upon the deformation of minerals: in Lister, G. S. et al (eds), The effect of deformation on rocks: Tectonophysics, 78, pp. 335-383.
- Hyndman, D. W., in press, Petrology of Igneous and Metamorphic Rocks, 2nd Edition: McGraw-Hill Book Co., New York, N.Y.
- _____, 1980, Bitterroot dome - Sapphire tectonic block, an example of a plutonic-core gneiss-dome complex with its detached supra-structure: Geological Society of America Memoir 153, pp. 427-443.
- Kerrich, R., Allison, I., Barnett, R. L., Moss, S. and Starkey, J., 1980, Microstructural and chemical transformation accompanying deformation of granite in a shear zone at Mieville, Switzerland; with implications for stress corrosion cracking and superplastic flow: Contributions in Mineralogy and Petrology, 73, pp. 221-242.
- Kerrich, R., Fyfe, W. S., Gorman, B. E. and Allison, I., 1977, Local modification of rock chemistry by deformation: Contributions in Mineralogy and Petrology, 65, pp. 183-190.
- LeForte, P., 1981, Manaslu leucogranite: a collision signature of the Himalaya a model for its genesis and emplacement: Journal of Geophysical Research, 86, pp. 10545-10568.

- Lister, G. S. and Price, G. P., 1978, Fabric development on quartz-feldspar mylonite: *Tectonophysics*, 49, pp. 37-78.
- Mattauer, M., Collot, B. and Van den Driessche, J., 1983, Alpine model for the internal metamorphic zones of the North American Cordillera: *Geology*, 11, pp. 11-15.
- Matthews, W. H., 1981, Early Cenozoic resetting of K-Ar dates and geothermal history of northern Okanogan Area, British Columbia: *Canadian Journal of Earth Sciences*, 18, pp. 1310-1319.
- McMillen, D. D., 1981, Structural geology and stratigraphy of a margin of the Okanogan dome, Okanogan County, Washington: *Regional Implications: Geological Society of America Abstracts with Programs*, 13, p. 96.
- Medford, G. A., 1975, K-Ar and fission track geochronometry of an Eocene thermal event in the Kettle River (west half) map area, southern British Columbia: *Canadian Journal of Earth Sciences*, 12, pp. 836-843.
- Miller, F. K. and Engels, J. C., 1974, Distribution and trends of discordant ages of the plutonic rocks of northeastern Washington and northern Idaho: *Geological Society of America Bulletin* 86, pp. 517-528.
- Monger, J. W. H., Price, R. A. and Trempleman-Kluit, D. J., 1982, Tectonic accretion and the origin of the two major metamorphic and plutonic belts: *Geology*, 10, pp. 70-75.
- Pardee, J. T., 1918, *Geology and mineral deposits of the Colville Indian Reservation, Washington*: U. S. Geological Survey Bulletin 677, 186 pp.
- Pitcher, W. S. and Berger, A. R., 1973, *The Geology of Donegal: a Study of Granite Emplacement and Unroofing*: Wiley-Interscience, N. Y., 435 pp.
- Platt, J. P. and Visser, R. L. M., 1980, Extensional structures in anisotropic rocks: *Journal of Structural Geology*, 2, pp. 397-410.
- Powell, M. and Powell, R., 1977, Plagioclase-alkali-feldspar geothermometry revisited: *Mineralogical Magazine*, 41, pp. 253-256.
- Ramsey, J. G. and Graham, R. H., 1970, Strain variation in shear belts: *Canadian Journal of Earth Science*, 7, pp. 786-813.
- Read, P. B. and Brown, R. L., 1981, Columbia River fault zone: southeastern British Columbia: *Canadian Journal of Earth Science*, 18, pp. 1127-1145.

- Rhodes, B. P., 1983, Kinematic analysis of mylonites from Spokane dome, a metamorphic core complex in northeastern Washington and northern Idaho: Geological Society of America Abstracts with Programs, 15, 5, p. 297.
- Rhodes, B. P. and Cheney, E. S., 1981, Low-angle faulting and the origin of Kettle dome, a metamorphic core complex in northeastern Washington: Geology, 9, pp. 366-369.
- Rinehart, C. D. and Fox, K. F., Jr., 1976, Bedrock geology of the Conconully quadrangle, Okanogan County, Washington: U. S. Geological Survey Bulletin 1402, 58 pp.
- _____ and _____, 1972, Geology of the Loomis quadrangle, Okanogan County, Washington: Washington Division of Mines and Geology Bulletin 64, 124 pp.
- Ross, J. V., 1975, A Tertiary thermal event in south-central British Columbia: reply: Canadian Journal of Earth Science, 12, pp. 899-902.
- _____, 1974, A Tertiary thermal event in south-central British Columbia: Canadian Journal of Earth Science, 11, pp. 1116-1122.
- Sibson, R. H., 1977, Fault rocks and fault mechanisms: Journal of Geological Society of London, 133, pp. 191-213.
- Snook, J. R., 1965, Metamorphic and structural history of "Colville batholith" gneisses, north-central Washington: Geological Society of America Bulletin 76, pp. 759-776.
- Stormer, J. C., Jr., 1975, A practical two-feldspar geothermometer: American Mineralogist, 60, pp. 667-674.
- Stormer, J. C., Jr., and Whitney, J. A., 1975, Geothermometry in sapphire granulite: an evaluation of two-feldspar and pyroxene methods (Abstr): Trans. Am. Geophys. Union, 56, pp. 446.
- Struik, L. C., 1981, A re-examination of the type area of the Devo-Mississippian Cariboo orogen, central British Columbia: Canadian Journal of Earth Science, 12, pp. 326-332.
- Tempelman-Kluit, D. J., 1979, Transported cataclasite, ophiolite and granodiorite in Yukon: Evidence of arc-continent collision: Geological Survey of Canada Paper 79-14, 27 pp.
- Tullis, J., Christie, J. M. and Griggs, D. T., 1973, Microstructures and preferred orientations of experimentally deformed quartzites: Geological Society of America Bulletin 84, pp. 297-314.

- Waters, A. C. and Krauskopf, K., 1941, Protoclastic border of the Colville batholith: Geological Society of America Bulletin 52, pp. 1355-1418.
- Watts, M. J. and Williams, G. D., 1979, Fault rocks as indicators of progressive shear deformation in the Guingamp region, Brittany: Journal of Structural Geology, 1, pp. 328-332.
- White, S. H., Burrows, S. E., Carreras, J., Shaw, N. D. and Humphreys, F. J., 1980, On Mylonites in ductile shear zones: Journal of Structural Geology, 2, pp. 175-187.
- White, S. H., 1979, Large strain deformation: report on a Tectonic Studies Group discussion meeting held at Imperial College, London on 14 November 1979: Journal of Structural Geology, 1, pp. 333-339.
- _____, 1976, The development and significance of mylonites: 25th International Geological Congress, Sydney, 1, p. 143.
- Whitney, J. A., Stromer, J. C., Jr. and Smith, R. L., 1975, Feldspar thermal histories for three post-metamorphic granites from the Georgia Piedmont: Geological Society of America Abstracts with Programs, 7, p. 549.